

***Ab initio* Dirac-Hartree-Fock calculations of chemical properties and *PT*-odd effects in thallium fluoride**

Harry M. Quiney

Department of Physics, Clarendon Laboratory, Parks Road, Oxford OX1 3PU, United Kingdom

Jon K. Laerdahl, Knut Fægri, Jr., and Trond Saue

Department of Chemistry, University of Oslo, P.O. Box 1033 Blindern, 0315 Oslo, Norway

(Received 29 September 1997)

The theory of *PT*-odd interactions relevant to existing experimental measurements of the hyperfine structure of TlF is reviewed. We outline a relativistic electronic structure theory based on single-particle four-component Dirac spinors, and implemented using methods borrowed from *ab initio* quantum chemistry. Numerical calculations are reported of the electronic structure of TlF, some of its chemical properties, and of its *PT*-odd electronic matrix elements. From these results, and from published experimental data, we derive bounds on the value of the electric dipole moment of the proton, d_p , the tensor coupling constant C_T , and the Schiff moment of the ^{205}Tl nucleus, Q , which are now the tightest available for these quantities. General issues regarding the calculation of the electronic structures of molecules containing heavy elements are also addressed. [S1050-2947(98)05002-1]

PACS number(s): 31.15.Ar, 31.30.Fv, 11.30.Er

I. INTRODUCTION

In his contribution to the 70th birthday celebrations of Einstein, Dirac analyzed the forms of the dynamical theories which are derived from Einstein's relativity principle [1]. The special theory of relativity, which is sufficient to describe the dynamics of atomic and molecular systems, requires that the laws of nature be independent of the position and velocity of the observer. Dirac noted that any change in the position and velocity of an observer can be constructed in a relativistically invariant way from a series of infinitesimal transformations which do not involve reflections in the space or time coordinates. He remarked that he could see no reason why the laws of nature need be invariant under space or time reflections, despite the fact that all the exact physical laws known at that time certainly did conform to this principle. This appears to be the first published demonstration that a valid physical law need not be symmetric with respect to space and time inversion. Purcell and Ramsey went further [2], and suggested that the validity of fundamental theories which are not symmetric with respect to spatial inversion (*P*-odd), time inversion (*T*-odd), or space *and* time inversion (*PT*-odd) could not be discounted without experimental evidence.

Following the theoretical and experimental insights of Lee and Yang [3], this evidence was obtained by Wu *et al.* [4], who observed that nuclear β decay is a *P*-odd process. This led to an extensive search for other phenomena which violate reflection symmetry, and to the development of theories to account for the phenomena. Of these, the first successful description of *P*-odd processes was supplied by the vector-axial theory of Feynman and Gell-Mann [5], which was an extension of Fermi's theory of β decay, but utilized mathematical techniques developed for the theory of quantum electrodynamics. This formed the basis for later developments, culminating in the standard model of the elec-

troweak interaction formulated by Glashow [6], Weinberg [7], and Salam [8]. Consequently, we now have a complete and renormalizable theory which accounts for *P*-odd interactions. From this theory may be derived an effective interaction which represents the interaction between electrons and the weak neutral currents within nuclei. This effective interaction, whose interaction strength is determined by the Fermi constant $G_F = 2.2 \times 10^{-14}$ a.u., may give rise to optical rotations in atomic metal vapors, energy differences between enantiomeric forms of chiral molecules, and nonvanishing transition probabilities between levels for which a dipole transition is strictly forbidden in the absence of the interaction [9,10]. Precision measurements of these tiny transition rates in the nuclear hyperfine structure of caesium vapor, combined with elaborate many-body calculations of the electronic structure of atomic caesium [11], provide compelling evidence of the internal consistency of the electroweak theory, and verification that the interaction strength is proportional to the so-called weak charge of the nucleus. In the most recent of these experiments [12], the detection of a nuclear anapole moment was reported, which results from a nuclear spin-dependent *P*-odd interaction.

Despite more than 40 years of experimental effort, however, there exists only one known example of a *T*-odd process, the decay of the neutral K^0 meson [13]. Such an interaction is not described by the standard electroweak model, and the origin of this effect is not understood, although several particle physics theories have been proposed to account for it [14]. Several of these theories also predict the existence of *PT*-odd interactions. On the grounds of symmetry, a *PT*-odd interaction caused by any mechanism would result in an experimental signature which is characteristic of an effective electric dipole moment (EDM). In the most straightforward interpretation of this property, a subatomic particle such as an electron or nucleon may possess a nonvanishing EDM, or a nucleus may acquire an EDM through

PT -odd nuclear forces. Alternatively, PT -odd weak neutral current interactions may give rise to couplings with external fields which resemble those caused by a static separation of charge. The consequences of the interaction of an elementary or nuclear EDM with an external electric field were first considered by Schiff [15], and are reviewed in Sec. II.

It was Sandars who first recognized that polar molecules containing heavy elements present an opportunity to detect the existence of an elementary or nuclear EDM [16]. He realized that spin-dependent interactions are enhanced by the internal electric field of a polar molecule, since spin-rotational states close in energy but opposite in parity would be mixed. Furthermore, there is a strong enhancement factor in heavy elements, necessitating a relativistic treatment of the electronic structure. Of all the possible candidates for study, TIF was chosen as the most suitable, because of its chemical stability, high polarity and polarizability, simple electronic structure, the enhancement of the interaction due to the ^{205}Tl nucleus, and the simple nuclear structure, which involves only a single unpaired proton (^{205}Tl) or proton hole (^{19}F). A series of experiments involving TIF have been performed [17–24], the results of which have been used to place bounds on fundamental nuclear PT -odd interaction constants. It is remarkable that these low-energy molecular physics experiments may act as sensitive probes of possible high-energy particle interactions beyond the standard electroweak model.

The interpretation of these experiments requires the calculation of matrix elements of effective PT -odd interaction operators, and it is with this task that the current paper is concerned. Attempts to extract the relevant electronic parameters from nonrelativistic electronic structure calculations have been made by Hinds and Sandars [19] and Coveney and Sandars [21], while nuclear structure calculations of PT -odd nuclear moments have been performed by Flambaum, Khriplovich, and Sushkov [25]. Recently, Parpia [26] has reported calculations of PT -odd effects in TIF using Dirac-Hartree-Fock wave functions. If calculations using moderate-sized basis sets of similar quality are compared, the results reported in Ref. [26] are in reasonable agreement with those obtained in this paper. However, we have been able to explore the limiting values of the PT -odd parameters by employing much larger basis sets, and have made a detailed study of the sensitivity of our results to basis set superposition errors, and to the variation in the electric field in the neighborhood of the ^{205}Tl nucleus. Unlike the calculations reported in Ref. [26], we have chosen the basis set parameters using a procedure which ensures accuracy of the molecular spinors in the critical region in the neighborhood of the ^{205}Tl nucleus. In this work, we calculate the relevant electronic structure parameters using relativistic quantum mechanics, and computational techniques borrowed from *ab initio* quantum chemistry. In order to perform these calculations to the required level of accuracy, this research has necessitated the development of new computational techniques, and represents a considerable advance in the state of the art of molecular electronic structure calculations.

We have already made a brief communication regarding *ab initio* calculations of the PT -odd electronic parameters in TIF [27], though no detail was given about how the calculations were performed. In this paper, we review in Sec. II the

PT -odd effective operators associated with the interaction of a proton EDM, d_p , with the internal electric and magnetic fields of the TIF molecule, the coupling constant of a nuclear tensor interaction, and the Schiff moment of ^{205}Tl . Although much of this material has already been published, these presentations [19,21] have been in the context of hybrid schemes involving relativistic atomic structure theory and nonrelativistic quantum chemistry. Here we collect together the essential theoretical material in order to formulate computational algorithms which are appropriate to our *ab initio* relativistic molecular structure calculations. In Sec. III, we outline those aspects of relativistic quantum theory which are relevant to our calculations, and describe the relativistic self-consistent field procedure. Algorithms are presented in Sec. IV which describe how the relevant PT -odd electronic parameters were extracted from our many-electron wave function for the TIF molecule. In order to assess the accuracy of our calculations, results are given together with a discussion in Secs. V and VI both for the PT -odd parameters and for chemical properties such as the calculated equilibrium bond length, harmonic force constant, and vibrational frequency. We also give details about how the fundamental PT -odd interaction constants are derived from our *ab initio* calculations and from the experimental data. The paper concludes with an assessment of the general relevance of our investigation to molecular structure calculations in Sec. VII. Some technical details have been presented in appendixes in order to avoid unnecessary interruption of the text.

II. EFFECTIVE PT -ODD NUCLEAR INTERACTIONS

A PT -odd effect would arise in an atom or a molecule through an effective interaction of the form

$$H_{\text{eff}} = -d\boldsymbol{\sigma}_N \cdot \boldsymbol{\lambda}, \quad (1)$$

where the nuclear spin operator is denoted by $\boldsymbol{\sigma}_N$, and $\boldsymbol{\lambda}$ is a unit vector in the direction of the molecular axis. We restrict our attention to the evaluation of coupling constants d , which arise due to the presence of a proton EDM, a weak neutral current interaction, or an nuclear EDM induced by PT -odd nuclear forces.

Nuclear magnetic resonance experiments have been performed on a molecular beam of TIF subjected to external electric and magnetic fields [17,18,20,22–24]. In these experiments, the hyperfine structure of TIF is measured with the external fields aligned both parallel and antiparallel. A nonzero frequency shift $\delta\nu$ in the hyperfine structure resulting from the reversal of one of the external fields is the experimental signature of a PT -odd interaction. The energy shift is related to the coupling constant in the effective interaction Hamiltonian by [20,24]

$$h\delta\nu = 4d|\langle \boldsymbol{\sigma}_N \cdot \boldsymbol{\lambda} \rangle|. \quad (2)$$

A nonvanishing coupling constant d may arise through a number of PT -odd processes, which we denote by the volume effect (d^V), magnetic effect (d^M), weak-neutral current effect, (d^T), and the Schiff moment effect (d^Q). In the following sections, effective operators are derived which establish the relations between these experimental parameters and

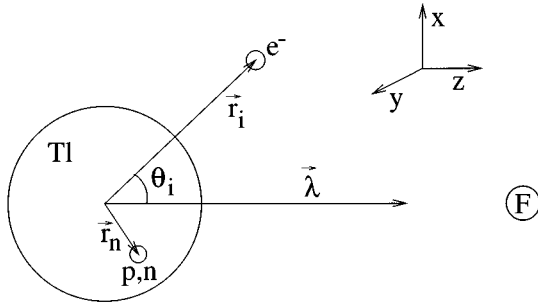


FIG. 1. Coordinate systems and notation for the thallium fluoride molecule. The position of electron i is specified by \mathbf{r}_i , and that of nucleon n , either a proton or a neutron, by \mathbf{r}_n . Each of these is defined with respect to a spherical polar coordinate system whose origin is located at the center of mass of the ^{205}Tl nucleus. The internuclear axis and the orientation of the spherical polar coordinate system which specifies the internal coordinates of the molecule is defined by the vector $\boldsymbol{\lambda}$, which for the sake of convenience we have aligned parallel to the z component of an external Cartesian coordinate system. The vector $\boldsymbol{\lambda}$ is directed toward the center of mass of the fluorine nucleus, labeled F in the diagram.

the proton electric dipole moment d_p , a weak neutral current coupling constant C_T , and the nuclear Schiff moment Q .

For the sake of clarity, we formulate our effective operators using labels adapted specifically for the TlF molecule. Any polar molecule MX , fulfilling the same nuclear structure restrictions satisfied by TlF, may be treated by similar methods, using the notational replacements $\text{Tl} \rightarrow M$ and $\text{F} \rightarrow X$. The wave function of the TlF system is denoted by Ψ , and is assumed to have the approximate form

$$\Psi = \Psi_N(\mathbf{r}_n) \Psi_F(\mathbf{r}_f) \Psi_e(\mathbf{r}_e) \Psi_R(\mathbf{r}_N, \mathbf{I}). \quad (3)$$

This comprises a nuclear wave function $\Psi_N(\mathbf{r}_n)$ for ^{205}Tl , a nuclear wave function $\Psi_F(\mathbf{r}_f)$ for ^{19}F , an electronic wave function $\Psi_e(\mathbf{r}_e)$, and a spin-rotational wave function $\Psi_R(\mathbf{r}_N, \mathbf{I})$. The coordinate system is defined in Fig. 1, where \mathbf{r}_i is the position of electron i in the coordinate system centered at the thallium nucleus, and \mathbf{r}_n is the position of nucleon n , either a proton or neutron, within the nucleus. The internuclear axis $\boldsymbol{\lambda}$ is aligned parallel to the external z axis. In our model of the TlF molecule, the nuclei are treated as classical charge distributions which generate external electrostatic fields in which the electrons move. The 90 electrons are point charges, whose coordinates we designate by $\mathbf{r}_e = (\mathbf{r}_1, \mathbf{r}_2, \dots, \mathbf{r}_{90})$. The electronic wave function $\Psi_e(\mathbf{r}_e)$ is an antisymmetrized product of single-particle spinors (Slater determinant) ψ_k , of the form

$$\Psi_e(\mathbf{r}_1, \mathbf{r}_2, \dots, \mathbf{r}_{90}) = \left(\frac{1}{90!} \right)^{1/2} \begin{vmatrix} \psi_1(\mathbf{r}_1) & \psi_2(\mathbf{r}_1) & \cdots & \psi_{90}(\mathbf{r}_1) \\ \psi_1(\mathbf{r}_2) & \psi_2(\mathbf{r}_2) & \cdots & \psi_{90}(\mathbf{r}_2) \\ \vdots & \vdots & \vdots & \vdots \\ \psi_1(\mathbf{r}_{90}) & \psi_2(\mathbf{r}_{90}) & \cdots & \psi_{90}(\mathbf{r}_{90}) \end{vmatrix}. \quad (4)$$

The electronic probability distribution is used to construct an adiabatic potential-energy surface on which the nuclei move.

The classical electrostatic equilibrium of the molecule is established by the condition that the forces on the nuclei vanish.

For a system of particles in electrostatic equilibrium, each member of which possesses a point charge and an EDM, there is no first-order interaction energy between a particular EDM and the electrostatic field generated by the other point charges. This restriction is often referred to as Schiff's theorem [15], and also holds for particles with a finite size if the charge and dipole distributions are identical. The details of the charge distribution within the atomic nuclei, however, are not included in the determination of the electrostatic equilibrium state, because the nuclear structure is determined by Coulomb forces between protons and non-Coulomb short-range interactions between nucleons. Due to the action of these non-Coulomb forces, different charge and dipole distributions may occur, and a nucleon EDM may experience a nonvanishing first-order interaction energy with the electric field generated by the electron density. This is called the volume effect, and will be discussed in Sec. II A. In a molecular system the electrostatic equilibrium may also be perturbed by magnetic forces, and this magnetic effect will be reviewed in Sec. II B. In Sec. II C we examine PT -odd effects which arise through an interaction between the electron density and the weak neutral current, and in Sec. II D we present the theory of the Schiff moment interaction, which is the result of PT -odd nuclear forces. Since the magnitudes of all of these interactions depend on the electron density in the neighborhood of the nuclear volume, a large enhancement of the effects is expected for molecules containing a heavy element such as thallium.

A. Volume effect

The volume effect is a first-order interaction between the EDM of the thallium nucleus and the electric field of the electrons under the assumption that the charge and dipole distributions in the nucleus differ. If q_n are the charges of the constituent nucleons in ^{205}Tl , q_i are the charges of the other particles in the system (electrons, and the ^{19}F nucleus), and $\mathbf{E}_{i,n}$ is the electric field at nucleon n due to charged particle i , then the average electrostatic force on the Tl nucleus is

$$\langle \mathbf{F} \rangle = \langle \Psi | \sum_{i,n} q_n \mathbf{E}_{i,n} | \Psi \rangle. \quad (5)$$

The first-order matrix element involving the interaction of this internal electric field with elementary nucleon dipoles is

$$\langle H_{\text{EDM}} \rangle = \langle \Psi | \sum_{i,n} -\mathbf{d}_n \cdot \mathbf{E}_{i,n} | \Psi \rangle. \quad (6)$$

Applying Gauss's theorem to the nuclear charge distribution, which we assume to be spherically symmetric, the electric field $\mathbf{E}_{i,n}$ may be written in the form

$$\mathbf{E}_{i,n} = -\frac{\mathbf{r}_i}{r_i^3} q_i [1 - \Theta(r_i, r_n)], \quad (7)$$

where the Heaviside step function $\Theta(r_i, r_n)$ is defined by

$$\Theta(r_i, r_n) = \begin{cases} 1 & \text{if } r_i < r_n \\ 0 & \text{if } r_i > r_n. \end{cases}$$

We actually require the force on a nucleon n due to a charged particle i . Consequently, the effective operator for the electrostatic force on a spherical ball of nucleon charge Q_n and of radius r_n , due to a particle i with charge q_i , is

$$\mathbf{F}_{i,n} = -\frac{\mathbf{r}_i Q_n q_i}{r_i^3} = -\frac{\mathbf{r}_i q_n q_i}{r_i^3} [1 - \Theta(r_i, r_n)]. \quad (8)$$

For the whole nucleus, we find that the force is

$$\langle \mathbf{F}_N \rangle = -\langle \Psi | \sum_{i,n} q_n q_i \frac{\mathbf{r}_i}{r_i^3} [1 - \Theta(r_i, r_n)] | \Psi \rangle, \quad (9)$$

and the interaction energy of the nucleon dipoles with the field is

$$\langle H_{\text{EDM}} \rangle = \langle \Psi | \sum_{i,n} q_i \frac{\mathbf{d}_n \cdot \mathbf{r}_i}{r_i^3} [1 - \Theta(r_i, r_n)] | \Psi \rangle. \quad (10)$$

These are just the Eqs. (5) and (6) of Ref. [19] with the conventional replacement of spherical tensors by their Cartesian equivalents. Following the notation of Ref. [19], we adopt the definitions

$$\langle \Psi_N | \sum_n q_n | \Psi_N \rangle = Z, \quad (11)$$

$$\langle \Psi_N | \sum_n q_n \Theta(r_i, r_n) | \Psi_N \rangle = Z \varrho_Z(r_i), \quad (12)$$

$$\langle \Psi_N | \sum_n \mathbf{d}_n | \Psi_N \rangle = D \boldsymbol{\sigma}_N, \quad (13)$$

$$\langle \Psi_N | \sum_n \mathbf{d}_n \Theta(r_i, r_n) | \Psi_N \rangle = D \boldsymbol{\sigma}_N \varrho_D(r_i), \quad (14)$$

where $\boldsymbol{\sigma}_N$ is a unit vector parallel to the nuclear spin, \mathbf{I} . The total nuclear charge is Z , ϱ_Z is the nucleon density, D is the total nuclear dipole moment, and ϱ_D is the nucleon dipole density. Integrating over the nuclear space, we obtain

$$\langle \mathbf{F}_N \rangle = -Z \langle \Psi_R \Psi_e | \sum_i q_i \frac{\mathbf{r}_i}{r_i^3} [1 - \varrho_Z(r_i)] | \Psi_R \Psi_e \rangle, \quad (15)$$

$$\langle H_{\text{EDM}} \rangle = D \langle \Psi_R \Psi_e | \sum_i q_i \frac{\boldsymbol{\sigma}_N \cdot \mathbf{r}_i}{r_i^3} [1 - \varrho_D(r_i)] | \Psi_R \Psi_e \rangle. \quad (16)$$

If we now ignore contributions from the protons in the F nucleus because of the localization of all the nucleons that comprise it, adopt $\boldsymbol{\lambda}$ as the internuclear unit vector, and substitute $q_i = -1$ a.u. for the electrons, we obtain

$$\langle \mathbf{F}_N \rangle = Z \langle \Psi_R \Psi_e | \boldsymbol{\lambda} \sum_i \frac{\cos \theta_i}{r_i^2} [1 - \varrho_Z(r_i)] | \Psi_R \Psi_e \rangle$$

$$= Z \langle \Psi_R | \boldsymbol{\lambda} | \Psi_R \rangle \langle \Psi_e | \sum_i \frac{\cos \theta_i}{r_i^2} [1 - \varrho_Z(r_i)] | \Psi_e \rangle, \quad (17)$$

$$\begin{aligned} \langle H_{\text{EDM}} \rangle &= -D \langle \Psi_R \Psi_e | (\boldsymbol{\sigma}_N \cdot \boldsymbol{\lambda}) \sum_i \frac{\cos \theta_i}{r_i^2} \\ &\quad \times [1 - \varrho_D(r_i)] | \Psi_R \Psi_e \rangle \\ &= -D \langle \Psi_R | \boldsymbol{\sigma}_N \cdot \boldsymbol{\lambda} | \Psi_R \rangle \langle \Psi_e | \sum_i \frac{\cos \theta_i}{r_i^2} \\ &\quad \times [1 - \varrho_D(r_i)] | \Psi_e \rangle. \end{aligned} \quad (18)$$

At the equilibrium internuclear separation, the electrostatic force on the nucleus vanishes. Setting $\langle \mathbf{F}_N \rangle = 0$, it follows from Eq. (17) that

$$D \langle \Psi_R | \boldsymbol{\sigma}_N \cdot \boldsymbol{\lambda} | \Psi_R \rangle \langle \Psi_e | \sum_i \frac{\cos \theta_i}{r_i^2} [1 - \varrho_Z(r_i)] | \Psi_e \rangle = 0, \quad (19)$$

since Z is just a number, and the left-hand side of Eq. (19) is just the projection of a vector proportional to $\boldsymbol{\lambda}$ in the direction of $\boldsymbol{\sigma}_N$, taken in the limit that the magnitude of the vector vanishes. Adding Eqs. (19) and (18), we obtain

$$\begin{aligned} \langle H_{\text{EDM}} \rangle &= -D \langle \Psi_R | (\boldsymbol{\sigma}_N \cdot \boldsymbol{\lambda}) | \Psi_R \rangle \langle \Psi_e | \sum_i \frac{\cos \theta_i}{r_i^2} \\ &\quad \times [\varrho_Z(r_i) - \varrho_D(r_i)] | \Psi_e \rangle \end{aligned} \quad (20)$$

at the equilibrium geometry. This is the expectation value of an effective operator which may be written in the form of Eq. (1), in which the electronic part of the matrix element in Eq. (20) forms part of the coupling constant d^V . Substituting the definitions of $\varrho_Z(r_i)$ and $\varrho_D(r_i)$ into Eq. (20), one obtains

$$\begin{aligned} \langle H_{\text{EDM}} \rangle &= -D \langle \Psi_R \Psi_N | \boldsymbol{\lambda} \cdot \sum_n \left(\frac{q_n}{Z} \boldsymbol{\sigma}_N - \frac{\mathbf{d}_n}{D} \right) | \Psi_R \Psi_N \rangle \\ &\quad \times \sum_i \int_0^{2\pi} d\varphi_i \int_0^\pi \sin \theta_i d\theta_i \\ &\quad \times \int_0^{r_n} r_i^2 dr_i \left(\psi_i^\dagger(\mathbf{r}_i) \frac{\cos \theta_i}{r_i^2} \psi_i(\mathbf{r}_i) \right). \end{aligned} \quad (21)$$

For small r_n , the nonvanishing component of the electronic part of Eq. (21) in the direction $\boldsymbol{\lambda}$, may be written

$$\lim_{r_n \rightarrow 0} \frac{2\pi r_n^2}{3} \left(\sum_i \frac{\partial}{\partial z_i} \psi_i^\dagger(\mathbf{r}_i) \psi_i(\mathbf{r}_i) \right) \Bigg|_{r_i=r_n} = r_n^2 X, \quad (22)$$

in which the quantity X is determined by the gradient of the electronic density at the center of mass of the nucleus, and z_i is the component of \mathbf{r}_i parallel to $\boldsymbol{\lambda}$. The equivalence of the electronic parts of Eqs. (21) and (22) may readily be estab-

lished by expanding each single-particle state, $\psi_i(\mathbf{r}_i)$, in a complete basis set centered at the ^{205}Tl nucleus.

Since the ^{205}Tl nucleus has a single unpaired $3s$ proton in the shell model, we set $D = d_p$, and the total nuclear EDM to $d_p \boldsymbol{\sigma}_N$. Integrating Eq. (21) over the nuclear coordinates, we obtain

$$\langle H_{\text{EDM}} \rangle = -d_p X R \langle \Psi_R | \boldsymbol{\sigma}_N \cdot \boldsymbol{\lambda} | \Psi_R \rangle, \quad (23)$$

where

$$R = \langle \Psi_N(\mathbf{r}_n) | \sum_n \left(\frac{q_n}{Z} - \delta_{n,3s} \right) r_n^2 | \Psi_N(\mathbf{r}_n) \rangle. \quad (24)$$

The factor $\delta_{n,3s}$ is included in the nuclear structure factor R to indicate that only the distribution function of the unpaired $3s$ proton is to be included in the evaluation of the nuclear EDM. Comparing Eqs. (23) and (1), we define the effective strength of the volume effect, d^V , by

$$d^V = d_p X R. \quad (25)$$

This formulation expresses the experimental coupling constant d^V in terms of d_p , which is the fundamental parameter of physical interest, an electronic structure factor X , whose value we will determine by *ab initio* Dirac-Hartree-Fock calculations, and a nuclear structure factor R . The principles involved in the calculation of X are derived from quantum electrodynamics, and the accuracy with which we may determine its value is limited solely by considerations of computational complexity.

B. Magnetic effect

Section II A discussed the possibility of observing the EDM of a charged particle subjected to the strong forces within a nucleus, which invalidates the assumption of electrostatic equilibrium inherent in Schiff's theorem [15]. Perturbation of the electrostatic equilibrium by magnetic interactions also raises the possibility of additional PT -odd effects. Here we investigate the interactions between the magnetic field of the electrons in TIF with a point nucleus with mass M_N , spin $\hbar/2$, magnetic moment $\mu_N \boldsymbol{\sigma}_N$, and EDM $d_p \boldsymbol{\sigma}_N$. Separate PT -odd operators may be derived from the interaction between the magnetic field and the nuclear current density and between the magnetic field and the nuclear magnetic moment. We denote these PT -odd interactions by H_M^1 and H_M^2 , respectively, and demonstrate that similarities in the form of these operators allow them to be amalgamated into a single effective magnetic interaction, which we denote by H_M .

The interaction of an EDM with the electromagnetic field of the electrons is given by [28,29]

$$\begin{aligned} & d_p c (\gamma_4 \gamma_5 \gamma_\mu \gamma_\nu)_N (\partial_\mu A_\nu - \partial_\nu A_\mu) \\ &= -d_p \beta_N \left[\boldsymbol{\sigma}_N \cdot \mathbf{E} - \boldsymbol{\sigma}_N \cdot \frac{\partial \mathbf{A}}{\partial t} + i \boldsymbol{\alpha}_N \cdot \mathbf{B} \right], \end{aligned} \quad (26)$$

in which the usual summation convention for repeated indices has been adopted. The components of the electromagnetic four-potential A_μ are derived from the partition of A

into a scalar part A^0 and a vector potential \mathbf{A} , so that $A = (A^0, \mathbf{A})$. Operators labeled with the subscript N refer to the nuclear coordinates. If we ignore the possibility of time-dependent vector potentials, then this is just the classical expression for the interaction between a dipole and an electromagnetic potential, and is the starting point for the derivation of H_M^1 . The Dirac Hamiltonian for the nucleus in the presence of this electromagnetic field may be written as

$$\begin{aligned} H &= c \boldsymbol{\alpha}_N \cdot (\mathbf{p} - Ze \mathbf{A}) + \beta_N M_N c^2 - Ze c A^0 \\ &\quad - d_p \beta_N (\boldsymbol{\sigma}_N \cdot \mathbf{E} + i \boldsymbol{\alpha}_N \cdot \mathbf{B}). \end{aligned} \quad (27)$$

where $c A^0$ is the scalar potential at the nucleus due to the electron distribution, \mathbf{E} is the associated electric field, and \mathbf{B} is the magnetic field due to the electron current.

In order to derive an effective operator proportional to $\boldsymbol{\sigma}_N \cdot \boldsymbol{\lambda}$, the Foldy-Wouthuysen transformation is employed. If we classify the constituent parts of H into odd and even operators \hat{O} and \hat{E} , we find that

$$\hat{O} = c \boldsymbol{\alpha}_N \cdot (\mathbf{p} - Ze \mathbf{A}) - i d_p \beta_N \boldsymbol{\alpha}_N \cdot \mathbf{B}, \quad (28)$$

$$\hat{E} = -Ze c A^0 - d_p \beta_N \boldsymbol{\sigma}_N \cdot \mathbf{E}. \quad (29)$$

The Foldy-Wouthuysen transformation of this operator is well known [30]. If we recall that the components of $\boldsymbol{\alpha}_N$ anticommute with β_N , retain only the lowest-order contributions in $1/M_N$ and d_p , and eliminate all terms involving products of \mathbf{A} and \mathbf{B} , we can write H as

$$\begin{aligned} H &= \beta_N \left(M_N c^2 + \frac{\hat{O}^2}{2M_N c^2} \right) + \hat{E} \\ &= \beta_N \left(M_N c^2 + \frac{p^2}{2M_N} - \frac{Ze \hbar}{2M_N c} \boldsymbol{\sigma}_N \cdot \mathbf{B} \right. \\ &\quad \left. + \frac{i d_p \beta_N [(\boldsymbol{\alpha}_N \cdot \mathbf{p})(\boldsymbol{\alpha}_N \cdot \mathbf{B}) - (\boldsymbol{\alpha}_N \cdot \mathbf{B})(\boldsymbol{\alpha}_N \cdot \mathbf{p})]}{2M_N c} \right) \\ &\quad - Ze c A^0 - d_p \beta_N \boldsymbol{\sigma}_N \cdot \mathbf{E}. \end{aligned} \quad (30)$$

The operator defined by Eq. (31) contains the usual parity-conserving terms, such as the rest mass energy, nonrelativistic kinetic and potential energies, and the coupling of a nuclear spin magnetic moment of magnitude $(Ze \hbar)/(2M_N c)$ with the magnetic field generated by the electronic current. As discussed below, this last term will give rise to H_M^2 , but since the ^{205}Tl nucleus has an internal structure which causes the magnitude of its experimental magnetic moment μ_N to differ from the prediction of the point-particle Dirac theory, we must treat PT -odd effects arising from this source separately. In addition, we obtain a PT -odd interaction Hamiltonian H_{EDM} of the form

$$H_{\text{EDM}} = d_p \left(\frac{i}{2M_N c} [(\boldsymbol{\alpha}_N \cdot \mathbf{p}), (\boldsymbol{\alpha}_N \cdot \mathbf{B})] - \beta \boldsymbol{\sigma}_N \cdot \mathbf{E} \right), \quad (32)$$

where the commutator is given by

$$[(\boldsymbol{\alpha}_N \cdot \mathbf{p}), (\boldsymbol{\alpha}_N \cdot \mathbf{B})] = (\boldsymbol{\alpha}_N \cdot \mathbf{p})(\boldsymbol{\alpha}_N \cdot \mathbf{B}) - (\boldsymbol{\alpha}_N \cdot \mathbf{B})(\boldsymbol{\alpha}_N \cdot \mathbf{p}). \quad (33)$$

The transformation Eq. (31) has effectively decoupled the large- and small-component contributions, because any product of four-component operators of the form $(\boldsymbol{\alpha}_N \cdot \mathbf{p})(\boldsymbol{\alpha}_N \cdot \mathbf{B})$ is block diagonal, with each 2×2 block involving operators of the Pauli two-component form $(\boldsymbol{\sigma}_N \cdot \mathbf{p})(\boldsymbol{\sigma}_N \cdot \mathbf{B})$. Considering only the interaction of the external electric field of the electrons, with the EDM of a point-like proton under the assumption of point charges at equilibrium, the term $-d_p \beta \boldsymbol{\sigma}_N \cdot \mathbf{E}$ has a vanishing expectation value because of Schiff's theorem. We can therefore write an equivalent effective operator in terms of the four-component operators of the form

$$H_M^1 = d_p \left(\frac{i}{2M_{NC}} [(\boldsymbol{\sigma}_N \cdot \mathbf{p}), (\boldsymbol{\sigma}_N \cdot \mathbf{B})] \right). \quad (34)$$

We now turn our attention to H_M^2 , which is an effective PT -odd Hamiltonian arising from the magnetic moment of the nucleus. The interaction between an intrinsic nuclear magnetic moment $\mu_N = g_N \mu_n$ and the magnetic field of the moving electrons has the form

$$H_\mu = -g_N \mu_n \boldsymbol{\sigma}_N \cdot \mathbf{B}, \quad (35)$$

where the nuclear magneton, μ_n is defined by

$$\mu_n = \frac{e\hbar}{2m_p c}, \quad (36)$$

and where the mass of the proton, m_p , is approximately $1836m_e$. This term is analogous to the third term in Eq. (31), in which the nuclear magneton is replaced by the experimental value of the nuclear magnetic moment of ^{205}Tl .

Following Schiff [15], we define the infinitesimal displacement operator Q , for a spin- $\frac{1}{2}$ particle whose electric dipole moment is $d_p \boldsymbol{\sigma}_N$, by

$$Q = \frac{d_p}{Ze\hbar} \boldsymbol{\sigma}_N \cdot \mathbf{p}. \quad (37)$$

Schiff pointed out that a dipole moment may be regarded as arising from the infinitesimal displacement of a point charge, and we show in Appendix A that the Hamiltonian H of the system can be written

$$H = \exp(iQ) H_0 \exp(-iQ) - i[Q, H_\mu] \quad (38)$$

to first order in d_p , where H_0 is that part of the Hamiltonian which is independent of electric dipole moments. This allows a determination of the eigenfunctions of the first term in H , ψ'_n , in terms of the eigenfunctions of H_0 , ψ_n^0 , through the relation

$$\psi'_n = \exp(iQ) \psi_n^0. \quad (39)$$

Since there is no dependence on d_p in the eigenfunctions of H_0 , there can be no correction, to first order in d_p , arising from the first part of the Hamiltonian. Here we are concerned with the interaction of a single-proton EDM, $d_p \boldsymbol{\sigma}_N$, which is present in the second part of H , and implicitly assume that interactions involving the EDM's of all other particles make no net contribution. This is possible because there is a single

unpaired proton in the shell model of the ^{205}Tl nucleus, and the closed-shell electronic structure of Tl eliminates all contributions from nonvanishing electron EDM's. To first order in d_p , the effective PT -odd interaction may be written in the form

$$\begin{aligned} H_M^2 &= -i\{QH_\mu - H_\mu Q\} \\ &= \frac{id_p g_N}{2Zm_p c} \{(\boldsymbol{\sigma}_N \cdot \mathbf{p})(\boldsymbol{\sigma}_N \cdot \mathbf{B}) - (\boldsymbol{\sigma}_N \cdot \mathbf{B})(\boldsymbol{\sigma}_N \cdot \mathbf{p})\}. \end{aligned} \quad (40)$$

Noticing that this is proportional to H_M^1 , we combine Eqs. (34) and (40), and generalize the result for an N -electron system to form the complete PT -odd magnetic interaction

$$H_M = id_p \left(\frac{1}{2M_{NC}} + \frac{g_N}{2Zm_p c} \right) \sum_j [(\boldsymbol{\sigma}_N \cdot \mathbf{p}), (\boldsymbol{\sigma}_N \cdot \mathbf{B})]_j. \quad (41)$$

The expectation value of this operator must be calculated using eigenstates which are not perturbed by the nuclear magnetic moment interaction, Eq. (35), a requirement which is satisfied by our Dirac-Hartree-Fock wave functions. Assuming that the center of mass of the molecule in which this nucleus is to be found is at rest, one may make the replacements

$$\mathbf{p} = - \sum_j \mathbf{p}_j, \quad (42)$$

$$\mathbf{B} = \sum_j \mathbf{B}_j, \quad (43)$$

$$\mathbf{B}_j = \left(\frac{\mathbf{r} \times \boldsymbol{\alpha}}{r^3} \right)_j. \quad (44)$$

Employing the identity

$$(\boldsymbol{\sigma} \cdot \mathbf{X})(\boldsymbol{\sigma} \cdot \mathbf{Y}) = \mathbf{X} \cdot \mathbf{Y} + i\boldsymbol{\sigma} \cdot (\mathbf{X} \times \mathbf{Y}), \quad (45)$$

and dropping terms independent of $\boldsymbol{\sigma}$, since they are not observable in the spin-resonance experiment which is the subject of this theoretical investigation, we find that

$$\begin{aligned} H_M &= d_p \left(\frac{1}{2M_{NC}} + \frac{g_N}{2Zm_p c} \right) \sum_j \boldsymbol{\sigma}_N \cdot \left\{ \mathbf{p} \times \left(\frac{\mathbf{r} \times \boldsymbol{\alpha}}{r^3} \right) \right. \\ &\quad \left. - \left(\frac{\mathbf{r} \times \boldsymbol{\alpha}}{r^3} \right) \times \mathbf{p} \right\}_j. \end{aligned} \quad (46)$$

By using a result presented in Appendix B, Hinds and Sanders showed [19] that the total magnetic interaction energy E_M , resulting from the combined effect of H_M^1 and H_M^2 , may be written in the form

$$\begin{aligned}
E_M &= \langle H_M^1 + H_M^2 \rangle \\
&= 2d_p \left(\frac{1}{2M_{NC}} + \frac{g_N}{2Zm_p c} \right) \\
&\quad \times \langle \Psi_R | \boldsymbol{\sigma}_N \cdot \boldsymbol{\lambda} | \Psi_R \rangle \sum_j \langle \psi_j | \left(\frac{\boldsymbol{\alpha} \times \mathbf{l}}{r^3} \right)_j | \psi_j \rangle_\lambda, \quad (47)
\end{aligned}$$

yielding an effective magnetic coupling constant d^M of

$$d^M = -2d_p \left(\frac{1}{2M_{NC}} + \frac{g_N}{2Zm_p c} \right) \sum_j \langle \psi_j | \left(\frac{\boldsymbol{\alpha} \times \mathbf{l}}{r^3} \right)_j | \psi_j \rangle_\lambda, \quad (48)$$

when we compare with the effective interaction in Eq. (1).

C. Weak-neutral current effect

Following Hinds, Loving, and Sandars [18] we write the most general nonderivative short-range parity-violating interaction between a nucleon and an electron on the form

$$\hat{H}_{\text{en}} = \sum_k \hat{H}_k = \sum_k iC_k (\bar{\psi}_n \Gamma_k \psi_n) (\bar{\psi}_e \Gamma_k \gamma_5 \psi_e), \quad (49)$$

where C_k is a coupling constant depending on the nature of the interaction, ψ_n here represents an electron-positron field operator, and $\bar{\psi}_n = \psi_n^\dagger \gamma_0$. The index k labels all vector (V), axial (A), scalar (S), pseudoscalar (P), and tensor (T) combinations Γ_k of the Dirac matrices $\{\gamma_\mu\}$. The combinations $k \in \{V, A\}$ are the P -odd interactions of the standard model of electroweak theory [14], and give rise to optical rotations in atomic metal vapors and transitions between states of opposite nominal parity. These phenomena are now well established by experiments whose precision has been refined by 25 years of continuous effort.

The combinations $k \in \{S, P, T\}$ yield PT -odd interactions which may induce effects characteristic of an EDM in atoms and molecules. If the odd-parity part of the interaction is restricted to electronic coordinates and the nuclear coordinates are treated nonrelativistically, the pseudoscalar interaction \hat{H}_P is eliminated. On symmetry grounds, the remaining scalar and tensor effective interactions \hat{H}_S and \hat{H}_T , respectively, assume the forms

$$\hat{H}_S = -\frac{d_S}{J} \mathbf{J} \cdot \mathbf{E}, \quad (50)$$

$$\hat{H}_T = -\frac{d_T}{I} \mathbf{I} \cdot \mathbf{E}, \quad (51)$$

where J is the total electronic angular momentum, M_J is the projection of J along the internuclear axis, I is the nuclear spin, \mathbf{E} is the external electric field, and the dipole coupling constants d_S and d_T are proportional to C_S and C_T , respectively. An experiment to determine C_S requires an atom or molecule with $J \neq 0$, while an experiment to determine C_T requires a nonzero nuclear spin $I \neq 0$. For a closed-shell molecule such as TIF, $M_J = 0$, so that $\langle \mathbf{J} \cdot \mathbf{E} \rangle = 0$, and there is no first-order contribution involving *only* the scalar interaction.

There is a nonvanishing first-order tensor interaction, however, because $I = \frac{1}{2}$ for ^{205}Tl and ^{19}F . If we assume that all second-order effects are smaller than those caused by first-order interactions, these selection rules enable experimental discrimination between the scalar and tensor electron-proton coupling constants. Since the tensor interaction is spin dependent in the shell model, the tensor coupling constant C_T derived from the TIF experiment contains only contributions from the unpaired proton. Evaluating the matrix element of \hat{H}_T in the TIF state function, Ψ , leads to an operator of the form Eq. (1) with a tensor coupling constant d^T defined by [21]

$$d^T = \sqrt{2} i C_T \sum_j \langle \psi_j | \varrho_p(\mathbf{r}_j) (\gamma_0 \boldsymbol{\alpha})_{j,\lambda} | \psi_j \rangle, \quad (52)$$

where $\varrho_p(\mathbf{r}_j)$ is the density of the unpaired proton in the ^{205}Tl nucleus at the electronic coordinate \mathbf{r}_j . Flambaum, Khriplovich, and Sushkov [25] showed that bounds on C_S also may be obtained from the TIF experiments, and this effect is considered briefly in Sec. VI D.

D. Schiff moment effect

Even if the nucleons do not possess an EDM, the nucleus may have a characteristic EDM due to a nonspherical charge distribution caused by PT -odd nucleon-nucleon interactions as shown by Coveney and Sandars [21]. The nuclear EDM d_N is written as a classical collection of point charges

$$\mathbf{d}_N = \sum_n q_n \mathbf{r}_n, \quad (53)$$

where the summation is over nucleons whose charge is q_n and whose position is \mathbf{r}_n . The interaction energy W of this charge distribution with the electric field due to the electrons, and the electric field at \mathbf{r}_N due to the electronic charge distribution $\mathbf{E}(\mathbf{r}_n)$, are given by

$$W = \sum_n q_n V_e(\mathbf{r}_n), \quad (54)$$

$$\mathbf{E}(\mathbf{r}_n) = -\nabla_e V_e(\mathbf{r}_n), \quad (55)$$

where $V_e(\mathbf{r}_n)$ is the electrostatic potential at \mathbf{r}_n . Following Coveney and Sandars [21], $V_e(\mathbf{r}_n)$ is expanded as a Taylor series about the center of mass of the nucleus \mathbf{r}_N , yielding the expansion for the interaction energy

$$\begin{aligned}
W &= ZV_e(\mathbf{r}_n) + \sum_n q_n (\mathbf{r}_n \cdot \nabla_e) V_e(\mathbf{r}_n) |_{\mathbf{r}_n = \mathbf{r}_N} \\
&\quad + \frac{1}{2} \sum_n q_n (\mathbf{r}_n \cdot \nabla_e)^2 V_e(\mathbf{r}_n) |_{\mathbf{r}_n = \mathbf{r}_N} \\
&\quad + \frac{1}{6} \sum_n q_n (\mathbf{r}_n \cdot \nabla_e)^3 V_e(\mathbf{r}_n) |_{\mathbf{r}_n = \mathbf{r}_N} + \dots \quad (56)
\end{aligned}$$

At equilibrium, the force on the nucleus, $\mathbf{F}_N = -\langle \nabla_N W \rangle$, vanishes. Setting $-\langle \nabla_N W \rangle = \langle \nabla_e W \rangle = 0$, it may be shown that

$$\nabla_e V_e(\mathbf{r}_N) = -\frac{1}{6Z} \sum_n q_n r_n^2 \nabla_e [\nabla_e^2 V_e(\mathbf{r}_n)]|_{\mathbf{r}_n=\mathbf{r}_N}. \quad (57)$$

This condition, which is valid if the system is in electrostatic equilibrium, is substituted into Eq. (56), yielding the effective perturbation

$$\hat{H}_N = \frac{1}{6} \left(\frac{3}{5} \sum_n q_n r_n r_n^2 - \frac{1}{Z} \sum_{n,n'} q_n q_{n'} r_n r_{n'}^2 \right) \nabla_e [\nabla_e^2 V_e(\mathbf{r}_N)]. \quad (58)$$

Taking the expectation value of \hat{H}_N in the state function Ψ leads to the effective operator

$$\hat{H}_{\text{eff}}^Q = -d^Q \boldsymbol{\sigma}_N \cdot \boldsymbol{\lambda}, \quad (59)$$

where [21]

$$d^Q = -6QX \quad (60)$$

$$Q = \frac{1}{6} \left[\frac{3}{5} \langle \Psi_N | \sum_n q_n r_n | \Psi_N \rangle - \frac{1}{Z} \langle \Psi_N | \sum_n q_n r_n^2 | \Psi_N \rangle \right. \\ \left. \times \langle \Psi_N | \sum_n q_n r_n / r_n^2 | \Psi_N \rangle \right]_{\lambda}. \quad (61)$$

The electronic integral X is defined by the volume effect parameter Eq. (22), and Q is the nuclear Schiff moment introduced in Refs. [25] and [31].

III. RELATIVISTIC ELECTRONIC STRUCTURE THEORY

The derivation of the coupled linear equations used in *ab initio* relativistic finite basis set calculations has over the years been presented by a number of authors, for example, Refs. [32,33], based on the early work of Refs. [34,35]. Here we review that development only to the extent that is necessary for the introduction of expressions and quantities which are essential for the discussions and derivations pertaining directly to the *PT*-odd effects studied by us. As most of these interactions involve the nuclear region, we discuss in particular the use of nuclear models of finite size as well as the solution of the Dirac-Hartree-Fock equations close to the nuclei.

A. Dirac-Hartree-Fock equations

For an external electromagnetic field consisting only of a time-independent scalar potential $V(\mathbf{r}) = -e\phi(\mathbf{r})$, the time-independent Dirac equation takes the form [32]

$$\{c\boldsymbol{\alpha} \cdot \mathbf{p} + \beta mc^2 + V(\mathbf{r})\} \psi_k(\mathbf{r}) = E_k \psi_k(\mathbf{r}). \quad (62)$$

Here $\psi_k(\mathbf{r})$ are four-component functions of position, four-spinors, with eigenvalues E_k . The 4×4 matrices $\boldsymbol{\alpha}$ and β are given by

$$\boldsymbol{\alpha}_q = \begin{bmatrix} 0 & \boldsymbol{\sigma}_q \\ \boldsymbol{\sigma}_q & 0 \end{bmatrix}, \quad \beta = \begin{bmatrix} \mathbf{I} & 0 \\ 0 & -\mathbf{I} \end{bmatrix}, \quad (63)$$

where $q = \{x, y, z\}$, $\boldsymbol{\sigma}_q$ are the Pauli spin matrices, and \mathbf{I} is the 2×2 unit matrix.

The solution of equations of this type forms the computational basis of the relativistic electronic structure theory of atoms and molecules. These solutions are classified as being of ‘‘positive-energy’’ type for $E_k > 0$, and ‘‘negative-energy’’ type for $E_k < 0$. For attractive potentials $V(\mathbf{r}) < 0$ of the type which most commonly occurs in electronic structure theory, the positive-energy solutions are further classified as square-integrable bound states if $-mc^2 < E_k < mc^2$. All other solutions belong to a continuum of states representing scattering in the external field. The problem of interpreting and handling negative-energy solutions has been described previously [32], and will not be pursued further here.

The Dirac equation is a single-particle equation, and the generalization of this equation to the many-particle case is not as straightforward as is the case in nonrelativistic theory. As a first step, the electronic Hamiltonian for N_{occ} particles may be written as a sum of Dirac operators for the individual particles

$$\hat{h}_D(\mathbf{r}_i) = c(\boldsymbol{\alpha} \cdot \mathbf{p})_i + \beta mc^2 + V(\mathbf{r}_i). \quad (64)$$

If the particles are assumed to interact through the Coulomb interaction, we obtain the Dirac-Coulomb operator

$$\hat{H}_{\text{DC}} = \sum_{i=1}^{N_{\text{occ}}} \hat{h}_D(\mathbf{r}_i) + \frac{1}{2} \sum_{i \neq j}^{N_{\text{occ}}} \frac{1}{|\mathbf{r}_i - \mathbf{r}_j|}. \quad (65)$$

The interpretation of this operator requires special care because of the presence of the negative-energy states. A second-quantized theory may be developed [32] which imposes the condition that these negative-energy states are not accessible under the circumstances prevailing in a molecular environment, leading to a computational scheme which closely resembles the practices encountered in nonrelativistic quantum chemistry. The total electronic energy within this theory is

$$E = \sum_{i=1}^{N_{\text{occ}}} \langle i | \hat{h}_D | i \rangle + \frac{1}{2} \sum_{i,j=1}^{N_{\text{occ}}} [(ii|\hat{g}|jj) - (ij|\hat{g}|ji)]. \quad (66)$$

Here Mulliken notation is used for the electron repulsion integrals, where

$$(ij|\hat{g}|kl) = \int \int \psi_i^\dagger(\mathbf{r}_1) \psi_j(\mathbf{r}_1) \frac{1}{|\mathbf{r}_1 - \mathbf{r}_2|} \psi_k^\dagger(\mathbf{r}_2) \psi_l(\mathbf{r}_2) d\mathbf{r}_1 d\mathbf{r}_2, \quad (67)$$

and $\psi_i^\dagger(\mathbf{r})$ is the Hermitian transpose of the four spinor, $\psi_i(\mathbf{r})$. For later convenience, we define

$$\psi_k(\mathbf{r}) = \begin{bmatrix} \psi_k^L(\mathbf{r}) \\ \psi_k^S(\mathbf{r}) \end{bmatrix}, \quad (68)$$

where $\psi_k^L(\mathbf{r})$ and $\psi_k^S(\mathbf{r})$ are two-spinor functions comprising, respectively, what is commonly denoted the ‘‘large components’’ and ‘‘small components’’ of $\psi_k(\mathbf{r})$. Here we neglect contributions from the Breit interaction, which is the lowest-order relativistic correction to the Coulomb interaction between electrons. It is assumed that this approximation may be invoked without introducing significant errors in our final calculations, because the properties in which we are inter-

ested depend mainly on valence electron amplitudes and that these will not be very sensitive to the magnetic and retardation effects described by the Breit interaction. We know from our calculations on atoms [36] that the self-consistent treatment of the Breit interaction contributes only a slowly varying effective potential, and we shall see in later sections that such a potential is unlikely to have a substantial effect on the numerical values of the PT -odd parameters which we calculate. In calculations of PT -odd effects in atoms, the authors of Ref. [29] showed that the Breit interaction contributes only a few percent to electron EDM parameters in TI, and we assess the sensitivity of our molecular calculations to be of a similar magnitude. Recently, the calculation of magnetic and retardation effects has been described and implemented in molecular electronic structure calculations [37]. The evaluation of matrix elements of the Breit interaction are intrinsically more expensive than those of the Coulomb interaction, and there is almost no experience of large-scale basis set calculations of the Breit interactions for molecules. However, the technology for such calculations now exists, and a detailed study of the effect of the Breit interaction in molecular structure calculations is planned as a development for the future.

If the energy of an electron at rest is defined to be c^2 atomic units, the matrix representation \mathbf{H} of the Dirac operator \hat{h}_D for an electron moving in the external field of N_{nuc} nuclei is

$$\mathbf{H} = \begin{bmatrix} \mathbf{H}^{LL} & \mathbf{H}^{LS} \\ \mathbf{H}^{SL} & \mathbf{H}^{SS} \end{bmatrix}. \quad (69)$$

Introducing the labels $\{\mu, \nu\}$ to denote the functions within the large- and small-component basis sets, the matrix elements of the blocks of \mathbf{H} are defined by

$$H_{\mu\nu}^{LL} = V_{\mu\nu}^{LL} + c^2 S_{\mu\nu}^{LL}, \quad (70)$$

$$H_{\mu\nu}^{SS} = V_{\mu\nu}^{SS} - c^2 S_{\mu\nu}^{SS}, \quad (71)$$

$$H_{\mu\nu}^{LS} = c \Pi_{\mu\nu}^{LS}, \quad (72)$$

$$H_{\mu\nu}^{SL} = c \Pi_{\mu\nu}^{SL}, \quad (73)$$

where

$$V_{\mu\nu}^{TT} = \left(\psi_{\mu}^T \left| \sum_{n=1}^{N_{\text{nuc}}} V_n(\mathbf{r}) \right| \psi_{\nu}^T \right), \quad (74)$$

$$S_{\mu\nu}^{TT} = (\psi_{\mu}^T | \psi_{\nu}^T), \quad (75)$$

$$\Pi^{T\bar{T}} = (\psi_{\mu}^T | \boldsymbol{\sigma} \cdot \mathbf{p} | \psi_{\nu}^{\bar{T}}). \quad (76)$$

The elements of the blocks $\mathbf{S}^{T\bar{T}}$, $\mathbf{V}^{T\bar{T}}$, and $\mathbf{\Pi}^{TT}$ are zero valued, $T=L$ or $T=S$, and $\bar{T} \neq T$. The density matrix \mathbf{D} is constructed in the block form

$$\mathbf{D} = \begin{bmatrix} \mathbf{D}^{LL} & \mathbf{D}^{LS} \\ \mathbf{D}^{SL} & \mathbf{D}^{SS} \end{bmatrix} \quad \text{where} \quad D_{\mu\nu}^{TT'} = \sum_{i=1}^{N_{\text{occ}}} c_{\mu i}^{T*} c_{\nu i}^{T'}. \quad (77)$$

Similarly, block matrices $\mathbf{G}^{TT'}$, which comprise \mathbf{G} , the matrix representation of the mean-field potential, may be evaluated. For explicit expressions see Ref. [33]. The components of the four-spinors may be expanded in a scalar basis sets [38], or directly in a two-spinor basis set [39]; these approaches are equivalent, provided that the *restricted* kinetic balance prescription (e.g., Ref. [40]) is adopted.

In these calculations, the *restricted* kinetic balance prescription [40] is enforced, in which the small-component basis set is generated by the action of the operator $(\boldsymbol{\sigma} \cdot \mathbf{p})$ on the large-component basis. This prescription removes the variational collapse problems that plagued early four-component calculations and guarantees that finite-dimensional representations of Dirac spinors tend toward exact representations in the limit of a complete set. For finite dimensions there is no ambiguity in the identity of individual members of the Dirac spectrum, and consequently there is a strict separation of the spectrum into its positive- and negative-energy branches. Stanton and Havriliak [41] demonstrate that solutions of the Dirac equation obtained in this way do not provide *rigorous* upper bounds to exact eigenvalues for a given potential, but it is our experience that the behavior is quasivariational if a finite nuclear model is adopted and uncontracted sets of Gaussian basis functions are used. The observed convergence behavior closely resembles that observed in nonrelativistic quantum chemistry as the dimension of the basis set is increased.

From these matrix expressions, the Dirac-Hartree-Fock approximation is obtained by replacing nonrelativistic Schrödinger operators by one-electron Dirac operators and constructing mean-fields from occupied positive-energy amplitudes. The Fock matrix \mathbf{F} is then defined as

$$\mathbf{F} = \mathbf{H} + \mathbf{G}. \quad (78)$$

In this matrix representation, the Dirac-Hartree-Fock approximation involves the solution of the generalized matrix eigenvalue equation

$$\mathbf{F}\mathbf{C} = \mathbf{e}\mathbf{S}\mathbf{C} \quad (79)$$

for the diagonal matrix \mathbf{e} , which contains the eigenvalues, and for \mathbf{C} , the matrix of spinor expansion coefficients. Since \mathbf{F} depends on \mathbf{D} , whose elements are constructed from the expansion coefficients of positive-energy four-spinors contained in \mathbf{C} , the Dirac-Hartree-Fock procedure involves the self-consistent solution of these coupled equations for the orbital energies and for the expansion coefficients of the spinors.

B. Finite nuclear effects

The nuclear point charge model, which is widely employed in nonrelativistic quantum chemistry, is not appropriate in systems involving heavy elements. Fortunately, the electronic properties of such systems are not strongly dependent on the details of the model which is adopted to represent the finite extent of the nuclear charge distribution. The simplest of these models is the uniform nuclear charge distribution, which represents the nucleus as a solid homogeneous sphere of charge. A more detailed model, the Fermi distribution, includes parameters derived from experiment, and is

widely used in relativistic atomic structure calculations. The most important nuclear parameter in electronic structure calculations is, however, the mean-square radius of the charge distribution, for which an empirical formula is available which depends only on the nuclear mass. In order to facilitate the evaluation of multicenter nuclear attraction integrals over our chosen electronic basis set, we adopt a Gaussian nuclear charge distribution whose mean-square radius matches the empirical data.

A normalized spherically-symmetric Gaussian charge distribution centered at \mathbf{P} may be written in the form

$$\begin{aligned} \varrho(\mathbf{r}_P) &= \varrho(r_P, \theta_P, \varphi_P) \\ &= 4\lambda \sqrt{\frac{\lambda}{\pi}} \exp(-\lambda r_P^2) Y_0^{*0}(\theta_P, \varphi_P) Y_0^0(\theta_P, \varphi_P) \end{aligned} \quad (80)$$

$$= \left(\frac{\lambda}{\pi}\right)^{3/2} \exp(-\lambda r_P^2), \quad (81)$$

where $(r_P, \theta_P, \varphi_P)$ is a spherical polar coordinate system whose origin is at \mathbf{P} , and λ is a positive constant which may be chosen so that the distribution reflects empirical root-mean-square values of particular nuclear radii. The parametric form for λ which was used in this study is

$$\lambda = 1.50 \times 10^{10} \left(\frac{0.529 \ 177 \ 249}{0.836A^{1/3} + 0.57} \right)^2, \quad (82)$$

where A is the nuclear mass number. The functional form given here, which includes the overlap distribution of normalized spherical harmonic functions, emphasizes the pragmatic choice of a Gaussian distribution as a model for the nucleus. Nuclear attraction integrals are, in this formulation, simply special cases of the more numerous electron-repulsion integrals which form the bulk of the computational effort in Dirac-Hartree-Fock calculations. In practice, the choice of a primitive Gaussian nuclear distribution is a good one, and may be refined by the inclusion of more functions, or of higher multipoles, if required.

From elementary electrostatics we may obtain the central field potential, $V(r_P)$, due to $\varrho(\mathbf{r}_P)$ for a nuclear charge Z from the relation

$$\begin{aligned} V(r_P) &= -Z \int_0^{2\pi} d\phi \int_0^\pi \sin(\theta) d\theta Y_0^{*0}(\theta_P, \varphi_P) Y_0^0(\theta_P, \varphi_P) \\ &\quad \times \left\{ \frac{1}{r_P} \int_0^{r_P} s^2 \varrho(s) ds + \int_{r_P}^\infty s \varrho(s) ds \right\} \\ &= -Z \left\{ \frac{1}{r_P} \int_0^{r_P} s^2 \varrho(s) ds + \int_{r_P}^\infty s \varrho(s) ds \right\}. \end{aligned} \quad (83)$$

After a little rearrangement, and dropping the subscript on r for convenience, we write the radial potential due to a Gaussian nucleus in the form

$$V(r) = -Z \left\{ \int_0^\infty s \varrho(s) ds + \frac{1}{r} \int_0^r s^2 \varrho(s) ds - \int_0^r s \varrho(s) ds \right\}$$

$$= V_0 + V_1 r + V_2 r^2 + \dots, \quad (84)$$

where

$$V_0 = -Z \int_0^\infty s \varrho(s) ds, \quad (85)$$

and the higher-order coefficients may be obtained simply by expanding $\varrho(s)$ and expanding term by term. We find that the explicit forms of these coefficients are

$$V_0 = -2Z \sqrt{\frac{\lambda}{\pi}}, \quad (86)$$

$$V_1 = 0, \quad (87)$$

$$V_2 = -\frac{\pi V_0^3}{12Z^2}. \quad (88)$$

The effect in which we are interested is strongly localized over the volume of the ^{205}Tl nucleus, so we may safely neglect all contributions to the potential from the electronic screening, since these add a positive constant to V_0 whose magnitude is much smaller than that of the bare nuclear value. In our calculations, we have used the value $\lambda = 1.388 \ 892 \ 520 \ 3 \times 10^8$ for ^{205}Tl , which corresponds to a root-mean-square radius of 1.0392×10^{-4} a.u., and yields $V_0 = -1.0771 \times 10^6$ a.u.

C. Solution of the Dirac equation for small r

In order to analyze the numerical behavior of the PT -odd interaction parameters, we need to know the form of the radial and angular parts of the solutions of the single-particle Dirac equation in the region of a heavy Gaussian nucleus. The electrostatic potential may be written in the form Eq. (84) and the radial form of the Dirac equation for the large and small components $P(r)$ and $Q(r)$ is

$$\begin{bmatrix} c^2 + V(r) - E & c \left(-\frac{d}{dr} + \frac{\kappa}{r} \right) \\ c \left(\frac{d}{dr} + \frac{\kappa}{r} \right) & -c^2 + V(r) - E \end{bmatrix} \begin{bmatrix} P(r) \\ Q(r) \end{bmatrix} = 0. \quad (89)$$

These radial solutions may be formed into atomic four-spinors $\psi_i(\mathbf{r})$, according to

$$\psi_i(\mathbf{r}) = \frac{1}{r} \begin{bmatrix} P_i(r) \chi_{\kappa, m}(\theta, \varphi) \\ i Q_i(r) \chi_{-\kappa, m}(\theta, \varphi) \end{bmatrix}, \quad (90)$$

in which $\chi_{\kappa, m}(\theta, \varphi)$ and $\chi_{-\kappa, m}(\theta, \varphi)$ are spin-angular two-spinors deduced from the more general functions $\chi_{jma}(\theta, \varphi)$, where

$$\chi_{jm, -1}(\theta, \varphi) = \begin{bmatrix} -\left(\frac{j+1-m}{2j+2} \right)^{1/2} Y_{j+1/2}^{m-1/2}(\theta, \varphi) \\ \left(\frac{j+1+m}{2j+2} \right)^{1/2} Y_{j+1/2}^{m+1/2}(\theta, \varphi) \end{bmatrix}, \quad (91)$$

$$\chi_{jm,1}(\theta, \varphi) = \begin{bmatrix} \left(\frac{j+m}{2j}\right)^{1/2} Y_{j-1/2}^{m-1/2}(\theta, \varphi) \\ \left(\frac{j-m}{2j}\right)^{1/2} Y_{j-1/2}^{m+1/2}(\theta, \varphi) \end{bmatrix}, \quad (92)$$

and $a = -\text{sgn}(\kappa)$. The functions $Y_{\nu}^{\mu}(\theta, \varphi)$ are spherical harmonic functions defined consistent with the conventions of Condon and Shortley [42]. These two-spinors are eigenfunctions of \mathbf{j}^2 with eigenvalue $j(j+1)\hbar^2$, the projection of \mathbf{j} in the z direction with eigenvalue $m\hbar$, and of the operator K , where

$$K = \begin{bmatrix} K' & 0 \\ 0 & -K' \end{bmatrix}, \quad (93)$$

$K' = -(2\mathbf{s} \cdot \mathbf{l} + 1)$, \mathbf{s} and \mathbf{l} are the usual spin and orbital angular momentum operators, and $K\psi_i(\mathbf{r}) = \kappa_i\psi_i(\mathbf{r})$. The allowed values of κ are $\kappa \in \{\pm 1, \pm 2, \dots\}$ and are associated with total angular momentum j , given by $j = (2|\kappa| - 1)/2$. In particular, $\kappa = -1$ corresponds to a $s_{1/2}$ state, $\kappa = 1$ to a $p_{1/2}$ state, and $\kappa = -2$ to a $p_{3/2}$ state. The m values are restricted to the half-integer values $-j \leq m \leq j$.

Spherical spinors of this form satisfy the identity

$$\boldsymbol{\sigma} \cdot \mathbf{p} \left[\frac{F(r)}{r} \chi_{\kappa, m}(\theta, \varphi) \right] = \frac{i}{r} \left[\frac{dF(r)}{dr} + \frac{\kappa F(r)}{r} \right] \chi_{-\kappa, m}(\theta, \varphi). \quad (94)$$

Expanding the functions $P(r)$ and $Q(r)$ as power series in r and classifying the solutions by $\kappa < 0$ and $\kappa > 0$, we obtain solutions whose characteristic features are summarized below.

Case I: $\kappa < 0$

$$\begin{aligned} P(r) &\approx r^{l+1} [p_0 + p_2 r^2] \\ Q(r) &\approx r^{l+2} [q_0 + q_2 r^2] \\ p_0/q_0 &= \frac{(2l+3)c}{V_0 + c^2 - E} \\ p_1 &= q_1 = 0. \end{aligned} \quad (95)$$

Case II: $\kappa > 0$

$$\begin{aligned} P(r) &\approx r^{l+1} [p_0 + p_2 r^2] \\ Q(r) &\approx r^l [q_0 + q_2 r^2] \\ p_0/q_0 &= -\frac{(V_0 - c^2 - E)}{(2l+1)c} \\ p_1 &= q_1 = 0. \end{aligned} \quad (96)$$

Note that in either case, p_0 is a constant which is determined by the spinor normalization condition, and that the ratio p_0/q_0 is, to a first approximation, independent of the bound-state eigenvalue. Setting $E = mc^2$ in the formulas above we obtain the approximate values $(p_0/q_0)_{-1} \approx -2620.1$ for $s_{1/2}$ spinors with $\kappa = -1$, and $(q_0/p_0)_{+1} \approx 2711.5$ for $p_{1/2}$ spinors with $\kappa = +1$.

IV. NUMERICAL EVALUATION OF PT -ODD ELECTRONIC PARAMETERS

A. Volume effect

The purpose of this section is to illustrate the origin of the most serious of our numerical problems in calculating PT -odd interaction parameters. By examining the analytic behavior of the molecular spinors in the neighborhood of the ^{205}Tl nucleus, we will find that one term in particular involves a numerical cancellation of contributions which may be reproduced accurately only if the atomic components of each spinor satisfy the analytic results for the p_0/q_0 ratios derived in Sec. III C.

The electronic structure factor X in Eqs. (25) and (60) is evaluated as the sum of single-particle contributions X_j according to the definitions

$$X = \sum_{j=1}^{N_{\text{occ}}} X_j, \quad (97)$$

$$X_j = \frac{2\pi}{3} [\nabla(\psi_j^\dagger(0)\psi_j(0))]_{\lambda}. \quad (98)$$

In practice, the X_j coefficients are calculated *directly* from the relation

$$\begin{aligned} X_j &= \lim_{r_n \rightarrow 0} \frac{1}{r_n^2} \left[\int_0^{2\pi} d\varphi_j \int_0^\pi \sin\theta_j d\theta_j \right. \\ &\quad \left. \times \int_0^{r_n} r_j^2 dr_j \psi_j^\dagger(\mathbf{r}_j) \frac{\cos\theta_j}{r_j^2} \psi_j(\mathbf{r}_j) \right]. \end{aligned} \quad (99)$$

In the limit $r_n \rightarrow 0$, this involves only the numerical values of the four-spinor amplitudes at $r=0$, which are readily deduced from the basis set expansion coefficients of the four-spinors, and angular factors which are determined analytically. The angular selection rules eliminate all contributions except from spinors of symmetry type $\omega = \frac{1}{2}$. Contributions to X_j from F-centered basis functions are negligible because the gradient of the electron density at the Tl nucleus is dominated by distortions in the Tl-centered atomic functions caused by molecular bond formation. All matrix elements involving F-centered basis function contributions are excluded in our calculations of X .

In order to analyze the numerical problems involved in the evaluation of X using our numerical techniques, it proves to be convenient to write each spinor as a *formal* one-center expansion of the form

$$\psi_j(\mathbf{r}) = |-1, m\rangle_j + |+1, m\rangle_j + |-2, m\rangle_j + \dots, \quad (100)$$

in which all explicit detail about the functional form of the expansion functions other than their symmetry properties is suppressed. The functions $|\kappa, m\rangle_j$ are atomic four-component spinors which satisfy the mean-field Dirac equation in the neighborhood of the Tl nucleus with molecular eigenvalue E_j , whose amplitudes are determined by the molecular calculation. For any diatomic molecule, we may select a representation for the degenerate Kramers pair of states belonging to a given molecular symmetry classification, ω , such that

the atomic symmetry types allowed in Eq. (100) are determined by a single value of the quantum number, $m = \pm \omega$, which is the projection of the total electronic angular momentum of $\psi_j(r)$ in the direction λ . These functions are defined with respect to a spherical polar coordinate system centered at the Tl nucleus, and take the form

$$|\kappa, m\rangle_j = \frac{1}{r} \begin{bmatrix} P_j^{\kappa, |m|}(r) \chi_{\kappa, m}(\theta, \varphi) \\ i Q_j^{\kappa, |m|}(r) \chi_{-\kappa, m}(\theta, \varphi) \end{bmatrix}. \quad (101)$$

The radial functions $P_j^{\kappa, |m|}(r)$ and $Q_j^{\kappa, |m|}(r)$ defined in Eq. (101) differ from the atomic solutions of the Dirac equation for spherically symmetric potentials defined in Eq. (90), since they depend on $|m|$ but are independent of the sign of m , for fixed κ . In principle, these functions may be obtained from the molecular spinors by projecting out all Tl-centered basis set components whose angular classification is (κ, m) from the single-particle molecular four-spinor, ψ_j , although we emphasize that we have no need to do this in practice. Atomic Tl-centered basis functions corresponding to symmetry types $\kappa = \{-1, +1, -2\}$ are the only ones which make any contribution to X , and all others are therefore excluded in the formal expansion in Eq. (100) for the sake of clarity.

The explicit forms of the Tl-centered atomic four-spinors for $m = \frac{1}{2}$ and small r are

$$\begin{aligned} | -1, \frac{1}{2} \rangle &= \begin{bmatrix} p_0^{-1} Y_0^0 \\ 0 \\ -i \sqrt{\frac{1}{3}} q_0^{-1} r Y_1^0 \\ i \sqrt{\frac{2}{3}} q_0^{-1} r Y_1^1 \end{bmatrix}, \\ | +1, \frac{1}{2} \rangle &= \begin{bmatrix} -\sqrt{\frac{1}{3}} p_0^{+1} r Y_1^0 \\ \sqrt{\frac{2}{3}} p_0^{+1} r Y_1^1 \\ i q_0^{+1} Y_0^0 \\ 0 \end{bmatrix}, \\ | -2, \frac{1}{2} \rangle &= \begin{bmatrix} \sqrt{\frac{2}{3}} p_0^{-2} r Y_1^0 \\ \sqrt{\frac{1}{3}} p_0^{-2} r Y_1^1 \\ -i \sqrt{\frac{2}{5}} q_0^{-2} r^2 Y_2^0 \\ i \sqrt{\frac{3}{5}} q_0^{-2} r^2 Y_2^1 \end{bmatrix}, \end{aligned} \quad (102)$$

where the state label j has been suppressed. The ratio of coefficients p_0^κ/q_0^κ may be deduced from Eqs. (95) and (96), and the value of either p_0^κ or q_0^κ may be deduced from the molecular amplitudes at $r=0$. It is sufficient to consider only the $m = +\frac{1}{2}$ spinors, since contributions to X from $m = -\frac{1}{2}$ spinors are identical in value on symmetry grounds.

The most critical contribution in the evaluation of X_j involves the atomic matrix element

$$X_j^{-1,1} = \lim_{r_n \rightarrow 0} \frac{1}{r_n^2} \langle -1, \frac{1}{2} | \frac{\cos \theta}{r^2} | +1, \frac{1}{2} \rangle_j, \quad (103)$$

in which the upper limit of radial integration is restricted by Eq. (99) to be r_n . Inserting the explicit form of the spinors into this matrix element, and multiplying by a factor of 2 for the contribution to X_j from its Hermitian conjugate $X_j^{1,-1}$, the contribution to X is

$$X_j^{-1,1} = -\frac{1}{3} [p_0^{-1} p_0^{+1} + q_0^{-1} q_0^{+1}]_j. \quad (104)$$

A similar treatment of the spinor contributions to X involving the atomic symmetry types $\kappa = -1$ and -2 , denoted by $X_j^{-1,-2}$, leads to the computational form

$$X_j^{-1,-2} = \frac{\sqrt{2}}{3} [p_0^{-1} p_0^{-2}]_j, \quad (105)$$

in which the r^2 dependence of the small-component amplitudes for $\kappa = -2$ eliminates all terms depending on q_0^{-1} and q_0^{-2} . All other combinations of symmetry type yield vanishing contributions to X .

For the ^{205}Tl nucleus, $V_0 \approx -1 \times 10^6$, and we may make the bound-state approximation $E \approx c^2$, resulting in the replacements

$$(V_0 + c^2 - E) \approx V_0, \quad (106)$$

$$(V_0 - c^2 - E) \approx V_0 - 2c^2. \quad (107)$$

Substituting these values into the relations connecting p_0^κ with q_0^κ , Eqs. (95) and (96), we find that

$$X_j^{-1,1} = -\frac{1}{3} [p_0^{-1} p_0^{+1}]_j \left[1 - \frac{V_0}{V_0 - 2c^2} \right]. \quad (108)$$

Since $|V_0| \gg 2c^2$, we expand the difference in the second bracket to find that

$$X_j^{-1,1} = \frac{1}{3} [p_0^{-1} p_0^{+1}]_j \frac{c^2}{V_0}. \quad (109)$$

The fact that we are able formally to expand Eq. (108) indicates that the direct evaluation of $X_j^{-1,1}$ must involve a strong numerical cancellation of large- and small-component contributions. For $V_0 \approx -1.0771 \times 10^6$ a.u. the cancellation of large- and small-component contributions involves two orders of magnitude, and can be achieved accurately only if our molecular four-spinors possess the correct $(p_0/q_0)^\kappa$ values for $\kappa = \{-1, 1\}$. In the nonrelativistic limit, only the p_0^κ values are involved in the calculation of X , and we may expect improved numerical stability of its numerical determination with respect to variations in the basis set.

B. Magnetic effect

In the calculation of the magnetic coupling constant, d^M , we define the intermediate computational quantities M and M_j , where

$$d^M = -2\sqrt{2}d_p \left(\frac{1}{2M_{Nc}} + \frac{g_N}{2Zm_p c} \right) M, \quad (110)$$

$$M = \sum_{j=1}^{N_{\text{occ}}} M_j, \quad (111)$$

$$M_j = \frac{1}{\sqrt{2}} \langle \psi_j | \left(\frac{\boldsymbol{\alpha} \times \mathbf{l}}{r^3} \right)_j | \psi_j \rangle_{\lambda}. \quad (112)$$

The one-electron operator involved in the evaluation of M_j may be written in the explicit matrix form

$$\frac{1}{\sqrt{2}} \frac{(\boldsymbol{\alpha} \times \mathbf{l})_z}{r^3} = \frac{1}{\sqrt{2}} \frac{i}{r^3} \begin{pmatrix} 0 & 0 & 0 & l_- \\ 0 & 0 & -l_+ & 0 \\ 0 & l_- & 0 & 0 \\ -l_+ & 0 & 0 & 0 \end{pmatrix}, \quad (113)$$

where we have assumed implicitly that $\boldsymbol{\lambda}$ is aligned parallel to the positive z axis. The angular momentum step operators have the usual definitions $l_{\pm} = l_x \pm il_y$.

Matrix elements of the electronic operator defined by Eq. (113) are evaluated as linear combinations of primitive Gaussian basis function integrals, using the property package of the HERMIT module in the DALTON program [43]. The numerical algorithms employed in that program are described by Saunders [44] and Helgaker and Taylor [45]. It was convenient to include exactly both one- and two-center contributions to the magnetic effect, so we have made no use of the reduction of Ref. [19] into one-center radial and angular parts.

C. Weak neutral current effect

The weak neutral current interaction coupling constant d^T may be related to the computational intermediates T and T_j by

$$d^T = -\sqrt{2}C_T T, \quad (114)$$

$$T = \sum_{j=1}^{N_{\text{occ}}} T_j, \quad (115)$$

$$T_j = -i \langle \psi_j | \varrho_p(\mathbf{r}_j) (\gamma_0 \boldsymbol{\alpha})_{j,\lambda} | \psi_j \rangle, \quad (116)$$

where the component of the matrix operator $\gamma_0 \boldsymbol{\alpha}$ in the direction of $\boldsymbol{\lambda}$ has the explicit form

$$\gamma_0 \boldsymbol{\alpha}_z = \begin{pmatrix} 0 & 0 & 1 & 0 \\ 0 & 0 & 0 & -1 \\ -1 & 0 & 0 & 0 \\ 0 & 1 & 0 & 0 \end{pmatrix}. \quad (117)$$

Like the magnetic effect, the matrix elements of this matrix operator are reduced to primitive integrals involving the scalar basis functions which constitute the individual components of the spinors. Since the function $\varrho_p(\mathbf{r})$ is localized at the ^{205}Tl nucleus, only one-center Gaussian basis function integrals are required, which were evaluated by elementary means. The evaluation was further facilitated by the use of an *explicit* 4×4 matrix representation of the effective one-electron operator in our numerical procedures, which ensures the correct coupling of components.

V. ATOMIC BASIS SET CONSTRUCTION

In the series of calculations reported here on the electronic structure of TlF, it was necessary to reconcile conflicting computational features of the relativistic self-consistent-field method. The main computational burden involved in the determination of the electronic structure of any molecule is weighted heavily toward the construction of the subvalence and valence orbitals which hold the molecule together, and not toward the core orbitals which contribute, to a good approximation, effective local potentials in which the valence electrons move. The values of the PT -odd parameters, however, depend almost wholly on amplitudes in the core region, and on contributions to molecular four-spinors from s - and p -type scalar Gaussian basis functions with exponent values larger than 10^5 . Since our calculations are based on the linear variation principle, these functions make a relatively minor contribution to the total electronic energy of the system.

The usual dependence on the Undheim-Hylleraas-Macdonald theorem [46], which plays a pivotal role in non-relativistic quantum chemistry, is not appropriate in the relativistic case, particularly if we are mainly interested in the electronic amplitudes near a heavy nucleus. For any atomic Gaussian basis set of finite dimension which is generated by nonlinear optimization of the energy with respect to the exponent set, the parameters derived by this procedure generally provide poor representations of the four-spinor amplitudes in the neighborhood of heavy nuclei. From a fundamental point of view, any finite basis set approximation of the bound-state eigenvalues of the Dirac equation need not be a strict upper bound to the exact values in *any* choice of basis [41]. This presents no problem of principle or practice: the calculations are variational in the sense that we seek a stationary point in the energy functional for a given basis set, and not an absolute minimum. We rely on the formal completeness of the basis in a given limit to justify the validity of the approximation scheme.

Since the Undheim-Hylleraas-Macdonald theorem is not a reliable guide to the construction of relativistic basis sets which are suitable for the calculation of the PT -odd electronic parameters, we devised a numerical test which provides a more sensitive measure of the quality of the spinors in the region of the Tl nucleus. In this region, the behavior of any molecular spinor is dominated by the local potential due to the nucleus, and we may apply the results of Eqs. (95) and (96) to the atomic components of each spinor. Since the electrostatic potential is spherically symmetric for small displacements from the center of mass of the Tl nucleus, it is simple to determine the ratio (p_0/q_0) defined by Eqs. (95) and (96) for each Tl-centered atomic symmetry type which

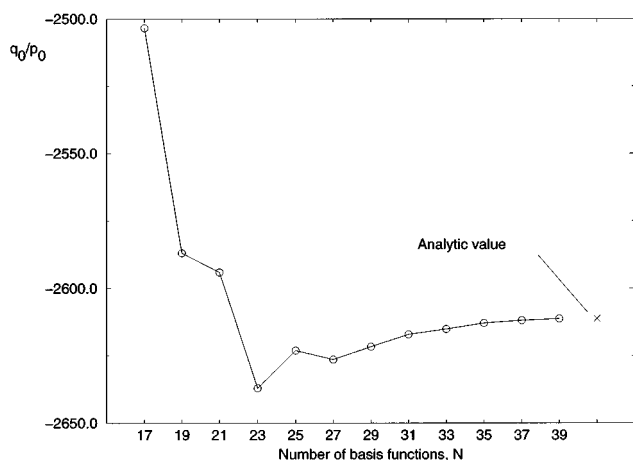


FIG. 2. The convergence of (q_0/p_0) with basis-set size for the $1s_{1/2}$ spinor of Tl^{80+} . The number of basis functions N in the even-tempered basis sets refers to Table I. The analytic value is calculated from Eq. (95).

contributes to a given four-spinor. In order to construct a basis which gives orbital eigenvalues of chemical quality, and which gives good representations of atomic spinors in the neighborhood of the nucleus, we constructed sets of Gaussian basis set exponents from carefully chosen geometric sequences.

Our preliminary tests concern the single-particle solutions for Tl^{80+} , in which the nucleus is modeled as a Gaussian charge distribution, and for which we derived analytic results in Sec. III C for the spinor amplitudes near the nucleus. The same basis set exponents $\{\lambda_i\}$ were used for the $\kappa = -1$ and 1 symmetry types, and are defined by the even-tempered prescription

$$\lambda_i = \alpha\beta_N^{i-1} \quad \text{where } i=1,2,\dots,N \quad (118)$$

for a radial basis of dimension N . The parameters $\alpha=0.04$ and $\alpha\beta_N^{N-1}=5.0\times 10^8$ for all the basis sets, and this range of functions is sufficient to ensure that we have a number of functions which are able to represent the spinors in the nuclear region, while retaining flexibility in the valence basis. The finite difference results from GRASP [47] are regarded as a numerical standard and are assumed to define the Dirac-Hartree-Fock limit for this system. From these calculations we find the energies $-3620.447\,145$ and $-930.962\,616$ a.u. for the $1s_{1/2}$ and $2p_{1/2}$ spinors, respectively. Inserting these values for the energies into Eqs. (95) and (96), we obtain the $(p_0/q_0)_\kappa$ Dirac-Hartree-Fock limit values, $(q_0/p_0)_{-1} = -2611.28$ and $(p_0/q_0)_{+1} = 2709.20$ for these two single-particle spinors. In Figs. 2 and 3 we display the convergence of $(q_0/p_0)_{-1}$ and $(p_0/q_0)_{+1}$ as the dimension N of the radial basis set, defined in Table I, is increased. It is very clear for both $\kappa = -1$ and $+1$ that the convergence is smooth, and that the ratios of the leading-order power-series coefficients tend toward the exact values dictated by Eqs. (95) and (96).

In the construction of basis sets for molecular calculations, we are restricted in the maximum radial dimension that we may use by practical considerations of the number of two-electron integrals which arise, which scales as the fourth

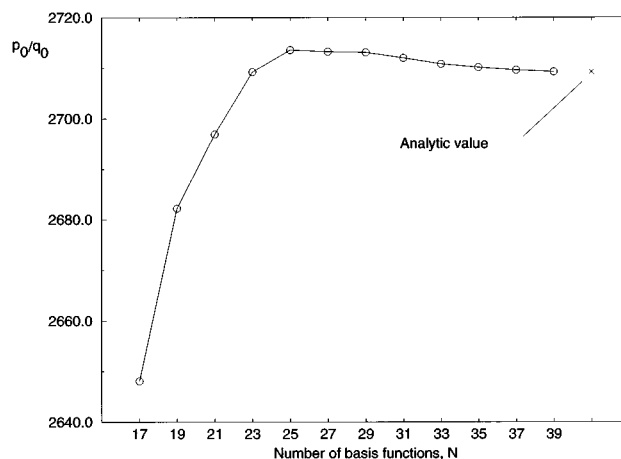


FIG. 3. The convergence of (p_0/q_0) with basis-set size for the $2p_{1/2}$ spinor of Tl^{80+} . The number of basis functions N in the even-tempered basis sets refers to Table I. The analytic value is calculated from Eq. (96).

power of the number of basis functions. We conducted a series of numerical tests on basis sets for atomic thallium, both using energy-optimized basis sets, and larger sets generated by systematic sequences of even-tempered functions. In the case of the even-tempered sets, the exponents for all symmetry types were selected from a single master list generated and labeled by the even-tempered prescription, Eq. (118). These basis sets are defined by the parameters displayed in Table II.

For comparison, an energy-optimized dual-family basis set was also used. In relativistic energy optimizations of basis set exponents [48], the relativistic contraction of electron density tends to favor the inclusion of basis functions with exponent values in the intermediate region at the expense of those with small values which represent the valence region and those with very high values representing the nuclear region. We replaced the four outer s (p) exponents of the energy-optimized basis set with a short sequence of six (seven) even-tempered exponents, in order to represent more accurately the valence region and polarization of the thallium atom. This basis set, labeled Tl-erg, is presented in Table III.

The even-tempered sets defined in Table II and the extended, energy-optimized basis set defined in Table III are of similar quality, if judged by the usual quantum-chemical yardstick of the total electronic energy. The basis sets Tl-erg and Tl-4 give total energies 10.8×10^{-3} and 11.9×10^{-3} a.u., respectively, above the Dirac-Hartree-Fock limit, which is $-20\,274.850\,644\,28$ a.u. In Table IV, we present orbital ei-

TABLE I. Even-tempered basis sets with N exponents defined by $\lambda_i = \alpha\beta_N^{i-1}$, where $i=1,2,\dots,N$. In order to give a comparable description of both the core and valence region $\alpha=0.04$ and $\alpha\beta_N^{N-1}=5.0\times 10^8$ for all the sets.

N	β_N	N	β_N	N	β_N
17	3.926	25	2.534	33	2.023
19	3.400	27	2.366	35	1.943
21	3.026	29	2.229	37	1.875
23	2.748	31	2.117	39	1.815

TABLE II. Even-tempered basis sets for the thallium atom used in this study. The notation $\{n_{1,l}:n_{2,l}\}$ denotes the first and last indices, respectively, of the basis sets for each atomic l value, with respect to the master list of N exponents defined by Eq. (118). In order to give a good description of both the valence and nuclear region the value of α_N is fixed at $\alpha_N=0.02$ and $\alpha\beta_N^{N-1}=5.0 \times 10^8$, for all N .

Basis	β_N	$\{N_k l_k\}$	$\{n_{1,l}:n_{2,l}\}$
TI-1	2.606	25s25p12d8f	(1:25,2:26,13:24,15:22)
TI-2	2.352	28s28p14d8f	(1:28,2:29,14:27,17:24)
TI-3a	2.165	31s31p15d8f	(1:31,2:32,16:30,19:26)
TI-3b	2.165	31s31p15d8f3g	(1:31,2:32,16:30,19:26,23:25)
TI-4	2.022	34s34p16d9f	(1:34,2:35,17:32,21:29)

genvalues, and the ratios $(q_0/p_0)_{-1}$ and $(p_0/q_0)_{+1}$, obtained using basis sets TI-4 and TI-erg, and compare them with the numerical values obtained using the finite difference program GRASP [47].

In all cases, the orbital eigenvalues obtained using basis sets TI-erg and TI-4 are in good agreement with the finite difference results. For spinors of $\kappa = -1$ symmetry, both basis set calculations generate values of $(q_0/p_0)_{-1}$ which are in satisfactory agreement with the finite difference values, with basis set TI-4 proving to have a slighter superior performance. However, for the symmetry-type $\kappa = +1$, the $(p_0/q_0)_{+1}$ values obtained using basis set TI-erg are wholly unsatisfactory. This deficiency indicates that the p -type functions in this basis set include insufficiently large exponents to describe the contraction of small-component electron density in $p_{1/2}$ four-spinors. The basis set labeled TI-4 does not suffer from this deficiency, because it contains several even-tempered functions whose exponents are sufficiently large to represent the structure of the spinors in the nuclear region. From the analytic solutions of Dirac spinors for small displacements from center of mass of the nucleus, it is clear that a small number of Gaussian-type functions is sufficient to represent atomic four-spinors in this region, provided that the exponent values are chosen to be sufficiently large that they are able to represent functional behavior dictated by the first few power-series coefficients. Clearly, the even-tempered set TI-4, has sufficient flexibility to be able to represent $|\kappa|=1$ atomic spinors in this region, while the energy-optimized basis, TI-erg does not. At the same time, we must include a sufficient number of diffuse basis functions so that our representation of the chemistry of TI is not sacrificed when we come to describe the bonding of TlF. Clearly, in many-electron systems where the valence spinors have several nodes and very small amplitudes near the nucleus, construction of a basis set which is suitable for the calculation of PT -odd effects is particularly difficult. Nevertheless, we find that our calculated p_0/q_0 ratios do converge with basis set size, and the largest basis set we have used, TI-4, is close to convergence. For these reasons, we will use the large even-tempered basis sets in the subsequent investigations of the structure of TlF.

The electronic structure in the vicinity of the fluorine nucleus is essentially nonrelativistic. For this reason we have adopted a nonrelativistic 9s6p basis set centered at the fluorine nucleus, augmented by two d -type functions to accom-

TABLE III. Relativistic dual-family 25s24p16d10f, energy-optimized basis set, TI-erg, where the functions in the valence region have been replaced with short sequences of even-tempered functions. The exponents are labeled λ , and the l values for which the exponents are employed, are denoted by $\{l_\lambda\}$.

λ	$\{l_\lambda\}$	λ	$\{l_\lambda\}$
50 980 195.85	(s)	18 626 562.61	(p)
11 526 467.50	(s)	3 444 971.589	(p)
3 216 581.844	(s)	800 643.0337	(p)
984 796.7808	(s)	215 991.5182	(p)
326 098.2911	(s)	65 027.984 47	(p)
114 874.8526	(s)	21 519.260 32	(p)
42 723.849 63	(s)	7 794.177 919	(p)
16 646.467 27	(s,d)	3 071.601 225	(p)
6760.138 769	(s,d)	1 302.202 853	(p)
2850.823 938	(s,d)	585.022 9722	(p,f)
1244.074 062	(s,d)	274.761 7212	(p,f)
558.424 386 9	(s,d)	133.303 1257	(p,f)
256.512 658 6	(s,d)	64.772 615 41	(p,f)
122.964 838 4	(s,d)	32.734 087 26	(p,f)
60.835 291 56	(s,d)	16.411 963 38	(p,f)
30.792 721 53	(s,d)	8.065 415 659	(p,f)
15.312 508 74	(s,d)	3.882 289 818	(p,f)
7.516 325 476	(s,d)	1.866 490 000	(p,f)
3.622 059 784	(s,d)	0.897 349 000	(p,f)
1.741 370 000	(s,d)	0.431 418 000	(p)
0.837 199 000	(s,d)	0.207 412 000	(p)
0.402 500 000	(s,d)	0.099 717 500	(p)
0.193 509 000	(s,d)	0.047 941 100	(p)
0.093 033 400	(s)	0.023 048 600	(p)
0.044 727 600	(s)		

modate the polarization of the atomic fluorine shells by the formation of molecular orbitals. The basis set have been optimized for the negative fluorine ion [49].

VI. RESULTS AND DISCUSSION

A. Chemical properties of TlF

In order to demonstrate that the basis sets used in this work contain sufficient variational freedom in the valence region to represent accurately the chemical bonding of the $^1\Sigma^+$ ground state of TlF, we completed a number of Dirac-Hartree-Fock (DHF) calculations of the electronic structure of TlF, and determined chemical parameters such as the equilibrium bond length (r_{eq}), harmonic force constant (k_0), and harmonic vibrational frequency (ν_0). All the thallium fluoride calculations reported in this paper were performed with the DIRAC program package [38], but, during the course of this study, a number of comparative calculations of both electronic structure and PT -odd effects were also performed using *independent* methods employed in the BERTHA program package [39]. Precise agreement was found between the results obtained by DIRAC and BERTHA if identical values of the speed of light, the internuclear separation, the nuclear structure parameters, and basis set exponents were used.

TABLE IV. Comparison of orbital eigenvalues (a.u.) and the ratios of power series coefficients, $(q_0/p_0)_{-1}$ and $(p_0/q_0)_{+1}$, for average of configuration calculations for the thallium atom. The values were obtained using the finite-difference program GRASP [47], the energy-optimized basis set, TI-erg in Table III, and the even-tempered basis set, TI-4 in Table II. The values $(q_0/p_0)_{-1}$ and $(p_0/q_0)_{+1}$ are given only for $|\kappa| = \pm 1$, because these are the symmetry types for which this parameter contributes most crucially to the PT -odd parameters.

	GRASP	$(p_0/q_0)^\kappa$	TI-erg	$(p_0/q_0)^\kappa$	TI-4	$(p_0/q_0)^\kappa$
1s	-3164.179 703 14	-2611.14	-3164.178 507 76	-2603.56	-3164.179 856 86	-2614.94
2s	-568.844 019 19	-2617.40	-568.843 413 13	-2609.92	-568.843 867 47	-2620.65
2p-	-544.949 523 40	2708.66	-544.948 178 72	2049.27	-544.949 394 10	2706.72
2p	-468.916 917 71		-468.916 523 51		-468.916 786 33	
3s	-138.363 359 38	-2618.43	-138.362 838 69	-2611.02	-138.362 796 18	-2621.02
3p-	-127.652 414 82	2709.64	-127.651 685 77	2050.17	-127.651 926 81	2707.65
3p	-110.528 050 13		-110.527 569 58		-110.527 517 15	
3d-	-93.083 780 78		-93.083 281 55		-93.082 690 12	
3d	-89.459 950 59		-89.459 531 60		-89.459 448 46	
4s	-32.292 565 14	-2618.68	-32.291 976 89	-2611.14	-32.291 764 88	-2618.42
4p-	-27.644 266 92	2709.87	-27.643 624 15	2050.39	-27.643 509 82	2708.01
4p	-23.427 452 61		-23.426 875 63		-23.426 681 20	
4d-	-15.843 560 55		-15.842 991 21		-15.842 694 12	
4d	-15.046 486 92		-15.045 943 24		-15.045 789 54	
5s	-5.619 084 82	-2618.74	-5.618 481 96	-2611.54	-5.618 591 89	-2616.96
4f-	-5.190 802 89		-5.190 222 59		-5.189 828 54	
4f	-5.014 787 63		-5.014 242 73		-5.013 963 12	
5p-	-3.985 138 93	2709.93	-3.984 530 12	2050.47	-3.984 681 01	2708.03
5p	-3.217 326 84		-3.216 750 75		-3.216 904 03	
5d-	-0.894 494 36		-0.893 956 43		-0.894 097 14	
5d	-0.806 172 61		-0.805 686 78		-0.805 809 00	
6s	-0.449 192 49	-2618.75	-0.448 861 31	-2611.67	-0.449 050 92	-2616.99
6p-	-0.211 355 73	2710.10	-0.211 057 58	2050.49	-0.211 255 32	2708.01
6p	-0.176 544 79		-0.176 253 10		-0.176 444 24	

A series of calculations were performed using basis set TI-3b at internuclear separations centered at the experimental value of the equilibrium bond length. The variation of the total energy with the bond length is displayed in Fig. 4, on which is superimposed the vibrational zero-point energy, assuming that TlF behaves like a harmonic oscillator. The corresponding nonrelativistic Hartree-Fock (HF) calculations were performed in the same basis using the program system,

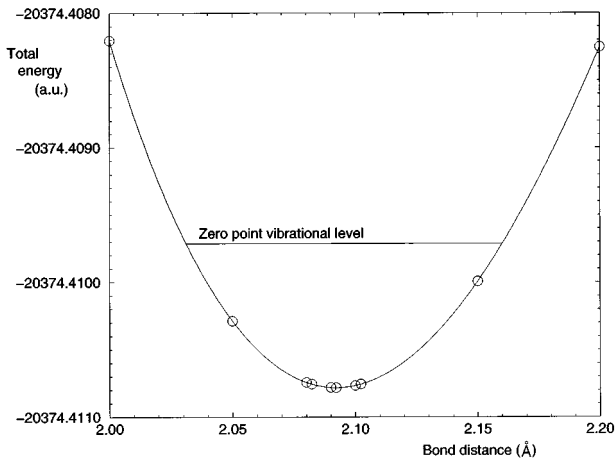


FIG. 4. The DHF potential-energy surface for thallium fluoride in the vicinity of the equilibrium bond length. The zero-point vibrational level is shown in the figure.

DALTON [43]. From these calculations, we deduced the spectroscopic parameters, the values of which are presented in Table V.

Since the DHF and HF calculations were performed in the same basis, we may interpret differences between the two calculations directly, as single-particle relativistic effects. Use of the Dirac single-particle Hamiltonian instead of the nonrelativistic Schrödinger operator causes a small expansion of the internuclear bond length. The better agreement of the HF and experimental r_{eq} values must be regarded as fortuitous, since the DHF and HF values do not include any electron correlation, which tends to stabilize the system.

TABLE V. Relativistic Dirac-Hartree-Fock (DHF) and nonrelativistic Hartree-Fock (HF) values of the equilibrium bond length r_{eq} , the force constant k_0 , and the harmonic vibrational frequency ν_0 for the $^1\Sigma^+$ ground state of thallium fluoride. The calculations have been performed with the basis set TI-3b in Table II. The results are compared with the experimental values (Expt.) quoted in Huber and Herzberg [62], and the force constants and vibrational frequencies are related through the reduced masses [62].

	r_{eq} (Å)	k_0 (N m ⁻¹)	ν_0 (cm ⁻¹)
DHF	2.092	227	470
HF	2.085	265	509
Expt.	2.084	233	477

TABLE VI. Variation of X_j , X , M , T (a.u.), and the electric field in the direction of λ , E_λ (a.u.) for calculations on thallium fluoride with basis sets for thallium defined in Table II. Spinors with $\omega=|m_j| \neq \pm \frac{1}{2}$ give no significant contributions to X , M , or T , and only the value of X_j for $\omega=\frac{1}{2}$ spinors with significant contributions to X is included in the main body of the table. The most significant atomic contributions to the molecular spinors are indicated. The values were obtained with an internuclear distance of 2.10 Å, which is close to the DHF equilibrium bond length. Powers of ten are given in parentheses.

j		Tl-1	Tl-2	Tl-3a	Tl-3b	Tl-4
1	$1s_{1/2}(\text{Tl})$	67.21	64.78	67.99	67.06	70.01
2	$2s_{1/2}(\text{Tl})$	-70.81	-90.16	-120.48	-88.50	-103.99
3	$2p_{1/2}(\text{Tl})$	-65.29	41.67	114.82	89.33	105.95
5	$2p_{3/2}(\text{Tl})$	43.10	46.10	51.64	42.75	45.22
6	$3s_{1/2}(\text{Tl})$	84.63	86.58	54.63	116.66	115.42
7	$3p_{1/2}(\text{Tl})$	-30.18	-26.66	-20.40	-63.18	-57.38
9	$3p_{3/2}(\text{Tl})$	-3.51	3.29	21.34	-2.49	0.92
15	$4s_{1/2}(\text{Tl})$	-27.50	-43.02	-105.04	-31.77	-34.45
16	$4p_{1/2}(\text{Tl})$	222.28	138.66	132.35	86.85	67.10
19	$4p_{3/2}(\text{Tl})$	72.14	82.53	110.28	81.35	79.13
25	$5s_{1/2}(\text{Tl})$	-463.71	-494.83	-585.03	-552.23	-520.10
33	$5p_{1/2}(\text{Tl})$	354.14	379.46	515.38	500.62	490.47
35	$5p_{3/2}(\text{Tl})$	457.26	472.86	507.69	496.57	466.22
36	$2s_{1/2}(\text{F})$	-143.83	-139.86	-145.31	-145.31	-150.46
42	$6s_{1/2}(\text{Tl}) + 2p(\text{F})$	-2365.12	-2330.64	-2421.13	-2420.49	-2495.50
43	$2p(\text{F})$	-34.26	-33.31	-38.30	-38.30	-43.03
45	$6s_{1/2}(\text{Tl}) + 2p(\text{F})$	5950.65	5884.52	6101.26	6103.63	6335.18
X		8098.38	8089.30	8491.22	8491.54	8746.63
M		13.64	13.62	13.66	13.66	13.63
T		-22.48	-22.42	-22.41	-22.41	-22.44
E_λ		-8.284(-4)	-1.359(-3)	-2.016(-3)	-7.123(-5)	-1.252(-3)

Both k_0 and ν_0 , however, are significantly better represented by DHF theory than by the HF results. On the basis of these observations, it would appear that the shape of the potential energy surface generated by the DHF calculations is a good approximation to the true Born-Oppenheimer function in the equilibrium region, except that it should be uniformly shifted to slightly shorter internuclear separations, and to an energy which is lower than the DHF equilibrium value by an amount equal to the correction to the DHF energy due to electron correlation and small corrections from the Breit interaction.

The derivation of the PT -odd parameter X defined in Sec. II A requires that the electronic structure calculations be performed in an electronic environment in which the net force on the Tl nucleus vanishes at the equilibrium bond length. For a *fully optimized* self-consistent-field wave function or a wave function at the Hartree-Fock limit, the Hellmann-Feynman force on the nucleus, \mathbf{F}^{HF} , defined by

$$\mathbf{F}^{\text{HF}} = -\langle \nabla V \rangle, \quad (119)$$

is equal to the physical force on the nucleus,

$$\mathbf{F} = -\nabla \langle H \rangle. \quad (120)$$

The equivalence of these quantities, and the requirement that the average force on the nuclei must vanish at the minimum value of the potential energy surface, is therefore a critical test of the quality of the basis set (see, e.g., Ref. [50]). Note

also that the qualification *fully optimized*, in this case, refers not only to the linear variational parameters, but also to the positions of the origins at which each basis function is centered. To investigate the completeness of our basis sets, we calculated the electric field at the thallium nucleus in the direction of λ due to all of the charges in the TlF molecule (E_λ), the results of which are given in Table VI. For the Tl-3b basis set we also calculated the electric field at different internuclear distances. These results are summarized in Table VII. In common with quantum-chemical experience, we find a strong basis set dependence on this quantity, even though the field was calculated at a bond distance of 2.10 Å, close to the minimum point of the DHF potential for all of the basis sets. If we compare the values of E_λ obtained for basis sets Tl-1, Tl-2, Tl-3a, and Tl-4, we find no obvious systematic behavior as the basis set dimension is increased, and no evidence that the value of E_λ is likely to vanish if we were to continue to augment the basis with more s -, p -, d -, or f -type functions. These calculations also show that the residual electric field is nearly constant with respect to variations in the internuclear separation, and that it does not vanish anywhere in the neighborhood of the equilibrium bond length. Any calculation with these basis sets therefore formally invalidates the assumptions built into the derivation of the PT -odd operators. Calculations with the energy optimized basis set Tl-erg give similar results, yielding an almost constant electric field of -0.0015 a.u. for all internuclear separations sampled by the classical ground-state vibrational amplitude.

TABLE VII. Variation in X , M , T , and E_λ (a.u.) with changes in the internuclear separation, r (Å), for calculations with the basis set Tl-3b in Table II. Powers of ten are given in parentheses.

r	2.00	2.05	2.10	2.15	2.20
X	8625.82	8586.42	8491.54	8361.80	8202.43
M	13.34	13.56	13.66	13.66	13.58
T	-23.19	-22.85	-22.41	-21.92	-21.37
E_λ	-6.070(-4)	-3.112(-4)	-7.123(-5)	1.226(-4)	2.780(-4)

The Hellmann-Feynman theorem may also be satisfied approximately in a calculation that is optimized only with respect to the linear variational parameters, if the basis set is ‘‘almost complete,’’ and particularly if it includes additional functions which are able to reflect the polarization of all atomic shells due to binding [51]. A nonrelativistic polarization function for atomic Tl is of g type, and we must include scalar functions of this type in the large component basis. The corresponding scalar h -type functions in the small component basis are introduced in order to satisfy the kinetic balance prescription, increasing the computational demands by a significant factor. It is for this reason that basis set Tl-3b was designed. It includes an atomic basis for Tl and F of good quality, with polarization functions for all atomic shells in order to restore the equilibrium of forces at the Tl nucleus in the region of the potential energy minimum. The effect on E_λ is dramatic, reducing its value by two orders of magnitude. With this basis, the Hellmann-Feynman force vanishes at an internuclear separation of 2.12 Å, close to the minimum point of the potential energy surface.

We also performed calculations of the spectroscopic parameters in Table V with the basis set Tl-3a in order to compare with the Tl-3b calculations. These calculations gave identical results to Tl-3b with the precision given in Table V showing that even if the polarization functions for the deep valence f spinors has large consequences for the electric field at the thallium nucleus it has a negligible effect on the spectroscopic properties at the DHF level. We did not calculate the spectroscopic parameters with the other basis sets, but from our experience with calculations of valence properties we expect that the position of the minimum of the potential-energy surface will vary by less than a few picometers for the basis sets which we have considered.

B. Calculation of PT -odd parameters

In the case of the PT -odd parameters, where there exists no experimental quantity with which we may compare to assess the accuracy of our calculations, it is imperative that a detailed study be made of the sensitivity of the parameters to details of the calculation. These details include the choice of basis set, basis set superposition errors, the electrostatic equilibrium condition, and the internuclear separation. In Table VI we summarize the calculated values for X , M , and T for the basis sets Tl-1–Tl-4. All the parameters are calculated at a bond length of 2.10 Å which is close to the equilibrium bond length for all the basis sets. The individual spinor contributions X_j are also given for all the spinors with a significant contribution to X . In Table VII we summarize the calculated PT -odd parameters at different internuclear distances for the Tl-3b basis set.

It can be seen from Table VI that of the PT -odd parameters, X is by far the most sensitive to the completeness of the basis set. This is not surprising, since X is determined from the spinor amplitudes at a single point. The parameters M and T , on the other hand, are derived from global integrals over the four-spinor amplitudes. In both cases, the integrals involve operators which very strongly weigh the region near the center of mass of the Tl nucleus, but the distribution of the integrand over these highly localized weight functions is sufficient to reduce the sensitivity of M and T to numerical errors in the spinor amplitudes. If we examine the data for all basis sets, we find that the values of M and T exhibit satisfactory stability with respect to the basis set, and the values seem to be converged with respect to basis set size to within 2% of the DHF limit. The total value of X in Table VI is less stable with respect to basis set, and in the analysis below we will summarize the numerical experiments we have performed to demonstrate that the final values are sufficiently stable for our purpose.

The two smallest basis sets Tl-1 and Tl-2 both give values of X of approximately 8100 a.u., the intermediate basis sets Tl-3a and Tl-3b yield a value of approximately 8500 a.u., and the largest basis set Tl-4 yields a value close to 8750 a.u. However, a spread in the results of this size is to be expected from the calculated values of p_0 and q_0 for the thallium atom, if the values for each basis set are inserted in Eq. (104). Of the basis sets, we expect Tl-4 to be the most accurate, both because it contains the largest number of functions, and because it gave the best results for the ratio p_0/q_0 in calculations of the structure of atomic Tl. The ratios are close to the finite difference results, and we expect X calculated from this basis set to differ by not more than a few percent from the DHF limit. It is interesting to note that while the total X is quite stable with basis set, the contributions for the core spinors vary substantially, and there is no apparent trend in the results. The difference between values derived from the basis sets Tl-3a and Tl-3b is particularly significant. As we saw in Sec. VI A, adding g -type polarization functions to the basis set changes the electric field at the thallium nucleus dramatically, and the Hellmann-Feynman theorem is satisfied, to a good approximation. The difference in the calculated electric field using basis sets Tl-3a and Tl-3b induces large changes in the values of the X_j contributions, including even a change of sign for one of the core spinors. At the same time the *total* value of X is only changed from 8491.22 to 8491.54 a.u., and the dramatic change in the electric field has almost no effect on the total value for this PT -odd property. The remarkable conclusion to be drawn from these observations is that cancellations in the core-orbital contributions are sufficiently precise that only the valence electrons

make any significant contribution to the parameters of interest, and that the valence spinors are quite insensitive to the addition of g -type polarization functions, and to the failure of the electric field at the Tl nucleus to vanish at the equilibrium when an incomplete basis set is used.

The causes of the significant fluctuations in the value of X as the basis set is changed are apparent if we examine in greater detail the orbital contributions, X_j . The most significant data are probably the X_j values for the spinors labeled 2 and 3. Molecular spinor ψ_2 is derived from the Tl $2s_{1/2}$ atomic spinor, while spinor ψ_3 is a weakly perturbed Tl $2p_{1/2}$ atomic spinor. These two orbitals are very close in energy to one another, but are widely separated in energy from all other TlF single-particle states. The spatial extent of both spinors is restricted to the region in the neighborhood of the Tl nucleus. Consequently, any nonspherical effective potential, arising either from the molecular environment, or due to an incompleteness in the basis set, mixes the atomic $2s_{1/2}$ and $2p_{1/2}$ atomic orbitals to form ψ_2 and ψ_3 in proportions which maintain the orthonormality of the molecular four-spinors. There is a delicate cancellation between contributions from ψ_2 and ψ_3 which arises through symmetry considerations, rather than from details of the effective molecular potential which causes the mixing of the core atomic orbitals to form the core molecular spinors. Similar, more elaborate cancellations of contributions occur for each of the shells of core atomic orbitals, which are mixed during bond formation to produce an orthonormal set of molecular spinors. The final values of X is derived almost wholly from the contributions from molecular spinors ψ_{42} and ψ_{45} , which are the valence orbitals formed by the formal transfer of an electron from the thallium atom to the fluorine atom when the ionic molecule TlF is formed. As a result, we conclude that the PT -odd parameters are sensitive mainly to the nonspherical effective potential which results from bond formation, and which determines the amplitudes of the valence spinors, rather than to details of the electric field at the center of mass of the Tl nucleus.

The most extreme example of sensitivity to the basis set arises if we calculate X using the energy optimized basis set, Tl-erg. This basis results in the lowest total energy for TlF of all the basis sets, but we find that $X = -25068$ a.u., which differs from the value obtained using our systematically constructed sets of functions by a factor of approximately -3 . The reason for this apparent discrepancy is that the functions which comprise Tl-erg have been optimized using total energy as the guiding criterion of quality. In the calculation of X , the cancellation between contributions from the components is subtle, and involves mainly the large components of $s_{1/2}$ functions, and the small components of $p_{1/2}$ functions. Clearly, the optimization procedure which generated the basis set Tl-erg does not maintain this delicate balance, despite its ability to represent single-particle quantities such as orbital eigenvalues. Extension of the basis to include more s - and p -type basis functions with large exponent values is required in order to improve the spinor representations near the nuclei; this extension would have a negligible effect on the calculated values of the chemical properties or the total energy.

From Eqs. (108) and (109) we may deduce the key feature of the numerical evaluation of X which explains why our

calculations appear to be so sensitive to the choice of basis set. Strong numerical cancellations in the large- and small-component parts of $X^{-1,1}$ are expected to occur, because every orbital contribution is calculated as a linear combination of terms of the type defined by Eq. (108) and this is also what we observe in our calculations. The Tl-4 calculations, for example, yield $X = 8747$ a.u., which is obtained from the sum of large- and small-component contributions, which are $149\,630$ and $-140\,883$ a.u., respectively. This imposes unusually stringent requirements on the basis set expansion of the spinor amplitudes in the neighborhood of the Tl nucleus, which the basis set Tl-erg fails to fulfill.

In summary, all of the basis sets except Tl-3b are of the same quality for the calculation of the electric field at the thallium nucleus, giving results that are not in agreement with the Hellmann-Feynman theorem and a field that does not vanish close to the equilibrium bond length. Of these basis sets, only Tl-erg gives a wholly unsatisfactory result for X , even though it yields the lowest total energy for TlF. Augmenting the basis set Tl-3a with extra polarization functions, resulting in Tl-3b, gives a basis set where the Hellmann-Feynman theorem is approximately satisfied. At the same time the difference in the total value of X for basis sets Tl-3a and Tl-3b is negligible, even though the core-orbital contributions X_j are sensitive to the residual electric field generated by Tl-3a. We conclude that accuracy of the total energy, orbital energies, and single-particle matrix elements such as the electric field at the nucleus provided insufficiently rigorous tests of basis set quality in the calculation of X . The basis set which is used must instead be able to reproduce finite difference amplitudes in the nuclear region and in particular give values for the ratio (p_0/q_0) close to the DHF limit.

One common situation in which basis set incompleteness has important effects in quantum chemistry is due to basis set superposition error. It is possible that the use of incomplete atom-centered basis sets could bias our calculations of the electric field and PT -odd parameters because of the asymmetric distribution of basis functions which this entails for TlF. Consequently, we investigated the effect of introducing ‘ghost’ functions, by copying the F-centered basis to the mirror point in space with respect to reflection in the Tl-nucleus coordinates. We also performed calculations of the PT -odd parameters for the Tl^+ ion in the unsymmetric basis set where the F ghost basis set was introduced at the position of the F atom in TlF. We concluded from this study that no value of X , M , and T is in error by more than 1% due to an unsymmetric distribution of the basis functions in the set. However this insensitivity parallels that which was observed when polarization functions were added to the basis: the changes in X_j for the core orbitals may be by as much as $10\text{--}20$ a.u., but the changes cancel due to the orthonormality constraints of the molecular spinors, so that only bonding contributions determine the total values.

In Table VII, we present the variation in X , M , T , and E_λ due to variations in r , calculated using basis set Tl-3b. The range of values for r in the table spans the whole region of the zero-point vibrational amplitude given in Fig. 4. To a good approximation, we find that X and E_λ vary linearly with internuclear separation although the agreement in the case of E_λ is not perfect, presumably because of basis set

incompleteness. Interestingly, M appears to have a weak, quadratic dependence on $r-r_{\text{eq}}$, achieving a maximum value close to the point at which the electric field vanishes. The average value of X and T over the ground-state vibrational amplitude is well-represented by its value at $r=r_{\text{eq}}$, because of the approximately linear dependence of these quantities on $(r-r_{\text{eq}})$. Strictly, one should take the vibrational average of X , M , and T , but the variation is either linear or so small over the vibrational amplitude that the value at $r=r_{\text{eq}}$ is sufficiently accurate for our purposes.

Given that we have established the insensitivity of the experimentally relevant parameters X , M , and T to variations in the bond length, basis set superposition error, polarization functions, and residual electric fields at the ^{205}Tl nucleus, we summarize our final results for our best basis set, TI-4 in Table VIII. We estimate that these values differ from the vibrationally averaged values calculated at the DHF limit by less than 8% for X , and 2% for M and T .

In order to make a comparison with earlier determinations of the PT -odd parameters, we performed a calculation of X by setting $c = 10\,000$ a.u., which is sufficiently large for us to obtain an estimate of X in the nonrelativistic limit, $c \rightarrow \infty$. In this case, the contribution to X_j from terms of the form defined by Eq. (104) involve no strong cancellation, because $q_0 \rightarrow 0$ for all atomic symmetry types. We find that the nonrelativistic value of X is 1130 a.u., and that its value is insensitive to variations in the basis set. The relativistic enhancement factor defined by Hinds and Sandars [19] is approximately seven. This is in good agreement with the analysis of Khriplovich [52], who suggested that its value should be 6.5 on the basis of atomic calculations. It is also in agreement with the estimate of the relativistic enhancement factor of Coveney and Sandars [21], who calculated its value by matching nonrelativistic molecular orbitals to relativistic atomic spinor amplitudes.

From Eq. (109), it is clear that the dominant contribution to the electronic matrix element from the nuclear density comes from V_0 , and not from the details of the nuclear shape. This implies that the use of a Gaussian nucleus, whose mean-square radius is chosen to match experimental parameters, is of sufficient accuracy for this problem, provided that V_0 matches more sophisticated estimates obtained, for example, from a Fermi distribution.

It is unlikely that the inclusion of electron correlation will have a significant effect on the calculated values of X , M , and T . The functional form and spatial domain of the operators associated with these quantities resembles those encountered in the calculation of NMR shielding tensors. For closed-shell systems and for the shielding tensor components associated with heavy nuclei, a self-consistent-field treatment of this property is usually reliable. This observation is invalidated for open-shell systems, in which core polarization plays a crucial role, or for the shielding tensors associated with light nuclei, in which the nuclear electrostatic field is unable to dominate the physical behavior. Of course, it is desirable that many-body effects be investigated in the context of the PT -odd interaction parameters, and is a study which we hope to perform in the future.

The most recent previous determination of X , M , and T was made by Coveney and Sandars [21] using nonrelativistic quantum chemistry methods and a procedure which matches

molecular orbitals to atomic spinors. In Table IX we compare our values for these parameters with those obtained in Ref. [21].

C. Determination of d_p , C_T , and Q

The calculation of d^M in Eq. (48) requires the use of some experimentally determined parameters, which we take to have the values $Z = 81$, $M_N = 205m_p = 3.764 \times 10^5$ a.u. and $g_N = 1.638$. From these data and the value of M from Table IX, we derive the relation

$$d^M = -1.923 \times 10^{-6} d_p \text{ a.u.} \quad (121)$$

The volume effect parameter d^V involves the nuclear structure factor R , which we take to be

$$R = 2.9 \text{ fm}^3 \quad (122)$$

$$= 1.036 \times 10^{-9} \text{ a.u.} \quad (123)$$

This value was obtained by Brown, and quoted in Ref. [21]. Calculations of the nuclear structure factor rely on model potentials derived mainly from experimental scattering data, and postulated forms for an effective nucleon-nucleon interaction. In view of these limitations of nuclear structure calculations, and the large cancellations involved in the evaluation of the difference between the mean-square charge and dipole densities in ^{205}Tl , the calculation of R presents the largest source of theoretical uncertainty in the calculation of the volume effect, within our physical model. Using the value of X from Table IX, we obtain

$$d^V = 9.062 \times 10^{-6} d_p \text{ a.u.}, \quad (124)$$

and note that d^M/d_p is about one-fifth of the magnitude of d^V/d_p , and has the opposite sign.

In order that the treatment of the volume and magnetic effects is consistent with the theoretical analysis, we have treated the sign of the EDM as significant, rather than taking the absolute value, as was done in Refs. [19] and [21]. We may quite simply adjust the most recent value of Coveney and Sandars [21] to conform with our treatment of the total effect arising due to d_p , yielding

$$\frac{|d_{\text{CS}}^V| + |d_{\text{CS}}^M|}{d_p} = 2.827 \times 10^{-6} \text{ a.u.} \quad (125)$$

$$= 3.505 \times 10^{18} \text{ Hz}/(e \text{ cm}), \quad (126)$$

which may be compared with the results of our calculations

$$\frac{d^V + d^M}{d_p} = 7.138 \times 10^{-6} \text{ a.u.} \quad (127)$$

$$= 8.851 \times 10^{18} \text{ Hz}/(e \text{ cm}). \quad (128)$$

By taking the ratio of our result with that of Coveney and Sandars, and adjusting the analysis of Ref. [24] by this factor, we obtain the revised proton EDM limit $d_p = (-1.5 \pm 2.5) \times 10^{-23} e \text{ cm}$. Revised limits for the tensor and Schiff

TABLE VIII. Four-spinor eigenvalues ε_j , and orbital contributions to X , M , and T (a.u.), obtained using our best basis set, Tl-4 for the 45 spinors with $m_j > 0$. The total electronic energy obtained in this basis set is $-20\,374.453\,554\,00$ a.u.; the total values of X , M , and T for all 90 electrons are, respectively, 8746.63 , 13.630 , and -22.442 a.u.

j	ε_j	X_j	T_j	M_j
1	-3164.193 799 39	70.01	-0.133	0.130
2	-568.857 226 60	-103.99	0.396	-0.097
3	-544.962 817 28	105.95	-0.516	0.014
4	-468.930 338 41	0.00	0.000	0.003
5	-468.930 045 53	45.22	0.000	0.181
6	-138.376 337 03	115.42	-0.425	0.107
7	-127.665 461 32	-57.38	0.284	-0.014
8	-110.541 590 98	0.00	0.000	-0.005
9	-110.540 606 03	0.92	0.000	-0.005
10	-93.096 748 69	0.00	0.000	0.001
11	-93.095 815 64	0.15	0.000	0.005
12	-89.473 748 47	0.00	0.000	0.000
13	-89.472 913 21	0.00	0.000	0.006
14	-89.472 547 02	-0.00	0.000	0.003
15	-32.305 529 50	-34.45	0.032	-0.105
16	-27.657 334 11	67.10	-0.289	-0.042
17	-26.185 188 41	-0.00	0.000	0.016
18	-23.441 576 19	0.00	0.000	-0.015
19	-23.439 498 37	79.13	0.000	0.284
20	-15.857 855 03	0.00	0.000	-0.001
21	-15.855 581 32	1.14	-0.000	0.034
22	-15.061 518 46	0.00	0.000	-0.001
23	-15.059 508 95	0.00	0.000	0.019
24	-15.058 550 63	0.01	0.000	0.016
25	-5.633 527 91	-520.10	1.203	-1.001
26	-5.205 766 38	0.00	0.000	0.000
27	-5.203 446 49	0.00	0.000	0.004
28	-5.202 269 08	0.02	-0.000	0.005
29	-5.030 266 94	0.00	0.000	0.000
30	-5.028 316 93	0.00	0.000	0.003
31	-5.027 000 32	0.00	0.000	0.003
32	-5.026 342 31	0.04	0.000	0.004
33	-4.000 323 54	490.47	-2.189	-0.159
34	-3.235 481 89	0.00	0.000	-0.042
35	-3.230 751 89	466.22	-0.011	1.720
36	-1.425 377 94	-150.46	0.289	-0.272
37	-0.914 925 11	0.00	0.000	-0.006
38	-0.909 683 59	0.68	-0.002	0.021
39	-0.828 466 23	0.00	0.000	-0.003
40	-0.823 986 34	0.55	0.003	0.053
41	-0.823 457 76	0.00	0.000	0.038
42	-0.560 884 17	-2495.50	5.284	-5.383
43	-0.511 923 24	-43.03	0.304	-0.027
44	-0.511 141 43	0.00	0.000	-0.050
45	-0.391 670 69	6335.18	-15.450	11.371

moment interaction constants C_T and Q , respectively, are obtained directly by taking ratios of the values of T and X in our work with those used in the analysis of [24]. The results are summarized in Table IX, and compared with the earlier results from the experiments of Ref. [24].

Our results for X , M , and T are larger than those obtained

in Ref. [21] by factors ranging between 3 and 5, and consequently our estimates of the bounds on d_p , C_T , and Q are tighter than previous limits by corresponding factors. There is a difference in our treatment of d_p , compared with that adopted in Refs. [19,21], since we have retained the signs of the interaction parameters X and M throughout our analysis,

TABLE IX. Numerical values of X , M , and T , and the PT -odd parameters d_p , C_T , and Q deduced from the TIF molecular beam experiments reported in Ref. [24].

	X (a.u.)	M (a.u.)	T (a.u.)	d_p (e cm)	C_T	Q (e fm ³)
[21,24]	2128	4.41	-4.12	$(-3.7 \pm 6.3) \times 10^{-23}$	$(-1.5 \pm 2.6) \times 10^{-7}$	$(2.3 \pm 3.9) \times 10^{-10}$
This work	8747	13.63	-22.44	$(-1.5 \pm 2.5) \times 10^{-23}$	$(-2.8 \pm 4.8) \times 10^{-8}$	$(5.6 \pm 9.5) \times 10^{-11}$

rather than working with the absolute values of the constituent parts. Nevertheless, these revised estimates, based on our electronic structure calculations and the experiments of Ref. [24], are the tightest available for the fundamental PT -odd interaction parameters d_p , C_T , and Q .

D. Other PT -odd interaction parameters

Limits on the PT -odd parameters d_p , C_T , and Q are not the only ones which could be deduced from our calculations, but they are the ones for which the TIF experiment provides the tightest limits. We shall now briefly consider other PT -odd interactions in the context of the TIF experiment.

The effective operator H_d corresponding to the interaction of an electron EDM d_e , with an external electric field \mathbf{E} , may be written in the alternative forms [29]

$$H_d = -d_e(\gamma_0 - I)\boldsymbol{\sigma} \cdot \mathbf{E} \quad (129)$$

$$= -2id_e c \gamma_0 \gamma_5 p^2. \quad (130)$$

These effective operators are equivalent in the sense that their expectation values are identical if calculated in exact eigenstates of a Dirac operator. In practice, Eq. (129) involves only the localized small component density, and \mathbf{E} is effectively dominated by the nuclear Coulomb field, so many-body contributions to \mathbf{E} may be neglected, to a good approximation [29]. It is found that agreement between matrix elements of this one-body approximation to Eq. (129) and those of the exact one-body form Eq. (130) is obtained at about the 3% level [29,53]. Either form of the operator is PT -odd in the electronic coordinates, and vanishes identically in first-order for a closed-shell molecule such as TIF. A nonzero interaction energy may, however, be obtained if we consider the *combined* first-order effects of H_d and the nuclear hyperfine interaction. Flambaum and Khriplovich [54] obtained limits on d_e from the TIF experiment by exploiting this combined effect, which were later refined in Ref. [24]. The limits obtained by this approach were summarized in Table 3 of the review article by Mårtensson-Pendrill [55], yielding $d_e = 1.7 \pm 2.9 \times 10^{-25} e$ cm. Our own calculations reduce this limit by a factor of about 4, since the theoretical values depend on quantities related to the calculation of X and M , and are related to the Coveney and Sandars values from which the limit is derived by the same factor. However, measurements on paramagnetic species which are directly sensitive to d_e yield even tighter limits and for example, electron EDM experiments on atomic thallium set limits of $(-3 \pm 8) \times 10^{-27} e$ cm on d_e , which is an order of magnitude tighter than the limits derived from the TIF experiment. This value also involves less theoretical uncer-

tainty, because of the more accurate treatment of electron correlation which is possible in atomic calculations of nuclear hyperfine structure.

In order to circumvent the use of nuclear hyperfine interactions in the determination of d_e , while exploiting the experimental sensitivity afforded by molecular experiments on spin-rotational structure, Sauer, Wang, and Hinds [56] devised a molecular spin interferometry experiment on the paramagnetic species $^2\Sigma$ YbF. The designed sensitivity of this experiment is $d_e \approx 10^{-28} e$ cm, which is far in excess of that which may be obtained from our calculations of TIF. These experiments involve the direct effect of H_d on the spin population of a molecular YbF beam, and requires the separate *ab initio* calculations of the open-shell structure of this radical for their interpretation. These calculations have now been performed, and will be reported elsewhere [53].

One may also derive values of the scalar interaction constant C_S defined in Eq. (49) by comparing the value of Q derived from the TIF experiment with nuclear structure calculations. Flambaum, Khriplovich, and Sushkov [25] have argued that nuclear interactions cause a significant enhancement of interactions involving \hat{H}_S . This effect is amplified by the fact that the nucleon contributions to C_S are additive, resulting in an enhancement of d^S compared to d^T of order A , the nuclear mass number. Based on our own calculations of X and the TIF experimental results, we estimate the limits on the scalar interaction to be $C_S = (-2 \pm 3) \times 10^{-6}$. While this provides a limit which is comparable with that obtained from direct measurements on atomic caesium, the tightest limit on this quantity is obtained by experiments on atomic thallium, which are an order of magnitude smaller; previous determinations of C_S are summarized in Table 3 of the review by Mårtensson-Pendrill [55]. Moreover, the atomic limits are determined solely by electronic structure calculations, and involve no uncertainties introduced by coupling to the nuclear structure. Since the ^{205}Tl nucleus has a single unpaired proton, whose mean-square charge and dipole distributions are very similar, nuclear structure uncertainties may introduce large theoretical errors in any value of C_S derived from the TIF experiment.

VII. CONCLUSION

There has been a rapid growth in the development of relativistic *ab initio* computational methods by which the electronic structure of molecules containing heavy elements may be calculated. Such approaches have been made feasible because of the resolution of difficulties associated with the finite basis set parametrization of the Dirac equation, developments in numerical algorithms to evaluate multicenter integrals over two-body interactions, and the steady increase in the power of electronic computers. In order to exploit

these resources better, *direct* computational algorithms for multicenter integral evaluation have been developed [38,39]. The processor power available from workstation computers is used in computationally intensive applications to reduce or eliminate the dependence on external storage devices. This approach was first investigated in the context of nonrelativistic calculations of the structures of extended molecules containing many nuclei [57]. It may be adopted without significant change to the calculation of molecules containing a few atoms and many electrons, which is the configuration characteristic of many interesting problems in heavy-element chemistry and molecular physics. Similarly, conventional many-body theory may be applied by adopting the direct algorithms of quantum chemistry to exploit basis sets of molecular four-spinors expanded in a finite basis set of Gaussian-type functions [49,58,59].

These technological developments have been applied to a physical problem which is of considerable importance to our understanding of fundamental interactions in nature, and for which only semiempirical computational approaches have existed in the past [55,60]. By deriving effective interaction Hamiltonians from parametrized, phenomenological models of *PT*-odd interactions, we have demonstrated that electronic interaction constants may readily be derived from the electronic four-component amplitudes which are obtained from DHF calculations. From the calculated parameters and from published experimental data, we have derived bounds on the value of the electric dipole moment of the proton, d_p , the tensor coupling constant C_T , and the Schiff moment of the ^{205}Tl nucleus, Q , which are the tightest available of these quantities.

From a computational point of view, the successful calculation of the electronic volume effect parameter X provides a demonstration that the DHF approximation, when formulated using basis sets which satisfy the restricted kinetic balance prescription, provides numerical values of the electronic amplitudes of high accuracy. The four-spinor amplitudes obtained using this approach may be used in much the same way as basis set approximations of spin-orbital amplitudes in nonrelativistic quantum chemistry. The methods developed here may be applied to problems beyond the narrow field of *PT*-odd interactions. The characteristic feature of all *PT*-odd operators considered here is the coupling that they involve between the electronic charge and current densities in the neighborhood of heavy nuclei with the electrostatic and magnetic fields associated with those nuclei. This is also a characteristic feature of the calculation of magnetic shielding and spin-spin coupling constants in systems containing heavy elements, and in the calculation of nuclear hyperfine constants in molecules. We expect that the numerical experience gained in the present study will be of immediate relevance in the study of these chemical properties using relativistic *ab initio* quantum chemistry.

ACKNOWLEDGMENTS

The British EPSRC is thanked for their financial support of H.M.Q. This work has also received support from the Norwegian VISTA program under Grant No. V6414, and fruitful exchanges between Oxford and Oslo have been financed by generous travel grants from the REHE program of

the European Science Foundation. The numerical results were obtained through the grant of computing time to J.K.L. from the Research Council of Norway (Programme for Supercomputing).

APPENDIX A: EFFECTIVE *PT*-ODD MAGNETIC MOMENT INTERACTION

Following Schiff [15], we define the one-particle operators

$$T = - \sum_i \frac{1}{2m_i} \nabla_i^2, \quad (\text{A1})$$

$$V_0 = \sum_{i>j} q_i q_j \int \int \rho_{C_i}(\mathbf{r}) \rho_{C_j}(\mathbf{r}') \frac{1}{|\mathbf{r}_i - \mathbf{r}_j + \mathbf{r} - \mathbf{r}'|} d^3 r d^3 r', \quad (\text{A2})$$

$$V = \sum_i q_i \int \rho_{C_i}(\mathbf{r}) \phi(\mathbf{r}_i + \mathbf{r}) d^3 r, \quad (\text{A3})$$

$$U = \sum_{i \neq j} q_i d_j \boldsymbol{\sigma}_j \cdot \int \int \frac{(\mathbf{r}_i - \mathbf{r}_j + \mathbf{r} - \mathbf{r}')}{|\mathbf{r}_i - \mathbf{r}_j + \mathbf{r} - \mathbf{r}'|^3} \times \rho_{C_i}(\mathbf{r}) \rho_{M_j}(\mathbf{r}') d^3 r d^3 r', \quad (\text{A4})$$

$$W = \sum_i d_i \boldsymbol{\sigma}_i \cdot \nabla_i \int \rho_{M_i}(\mathbf{r}) \phi(\mathbf{r}_i + \mathbf{r}) d^3 r, \quad (\text{A5})$$

where $\rho_{C_i}(\mathbf{r})$ is the charge density of particle i , $\rho_{M_i}(\mathbf{r})$ is its electric dipole moment density, d_i is its electric dipole moment, q_i is its charge, m_i is its mass, and $\phi(\mathbf{r}) = cA^0$ is the electrostatic potential at \mathbf{r} . The electric dipole moment associated with particle i is in the direction $\boldsymbol{\sigma}_i$. All second- and higher-order effects involving dipole-dipole interactions are neglected.

Schiff demonstrates that the Hamiltonian of the system, H , can be written in the form

$$H = \exp(iQ) H_0 \exp(-iQ) + \frac{1}{2} [Q, [Q, H_0]] + \dots, \quad (\text{A6})$$

where Q is defined in Eq. (37), and H_0 is the part of H independent of any EDM's. In the present case, $H_0 = T + V_0 + V + H_\mu$. Furthermore,

$$i[Q, V_0] = U', \quad (\text{A7})$$

$$i[Q, V] = W', \quad (\text{A8})$$

where U' and W' are constructed from U and W by replacing the dipole density $\rho_{M,i}(\mathbf{r})$ by the charge density $\rho_{C,i}(\mathbf{r})$. Since we have assumed that the particles are pointlike and that Q involves only the coordinates of a single proton, we find that $U - i[Q, V_0] = 0$ and $W - i[Q, V] = 0$. To first order in d_p , the nonvanishing parts of H may be written in the form

$$H = H_0 + i[Q, H_0] + (U - i[Q, V_0]) + (W - i[Q, V]) - i[Q, H_\mu] \quad (\text{A9})$$

$$= \exp(iQ)H_0\exp(-iQ) - i[Q, H_\mu], \quad (\text{A10})$$

as required.

APPENDIX B: EFFECTIVE *PT*-ODD MAGNETIC FIELD INTERACTION

In order to derive an effective operator for the magnetic interactions, Hinds [61] employed the operator identity

$$\begin{aligned} \mathbf{p} \times \left(\frac{\mathbf{r} \times \boldsymbol{\alpha}}{r^3} \right) - \left(\frac{\mathbf{r} \times \boldsymbol{\alpha}}{r^3} \right) \times \mathbf{p} &= (\mathbf{p} \cdot \boldsymbol{\alpha}) \frac{\mathbf{r}}{r^3} - \frac{\mathbf{p} \cdot \mathbf{r}}{r^3} \boldsymbol{\alpha} + \frac{\mathbf{r}}{r^3} (\boldsymbol{\alpha} \cdot \mathbf{p}) \\ &\quad - \boldsymbol{\alpha} \frac{\mathbf{r} \cdot \mathbf{p}}{r^3}. \end{aligned} \quad (\text{B1})$$

In order to reduce this operator to a computationally convenient form, we make use of the relations

$$(\boldsymbol{\sigma} \cdot \mathbf{A}) \boldsymbol{\sigma} = \mathbf{A} + i \boldsymbol{\sigma} \times \mathbf{A}, \quad (\text{B2})$$

$$\boldsymbol{\sigma} (\boldsymbol{\sigma} \cdot \mathbf{A}) = \mathbf{A} - i \boldsymbol{\sigma} \times \mathbf{A}, \quad (\text{B3})$$

$$(\boldsymbol{\sigma} \cdot \mathbf{A})(\boldsymbol{\sigma} \cdot \mathbf{B}) = \mathbf{A} \cdot \mathbf{B} + i \boldsymbol{\sigma} \cdot (\mathbf{A} \times \mathbf{B}), \quad (\text{B4})$$

$$\mathbf{R} = \frac{\mathbf{r}}{r^3}, \quad (\text{B5})$$

which are valid for arbitrary spin-independent operators \mathbf{A} and \mathbf{B} . Substituting them into the defining equation, we have

$$\begin{aligned} \mathbf{p} \times (\mathbf{R} \times \boldsymbol{\alpha}) - (\mathbf{R} \times \boldsymbol{\alpha}) \mathbf{p} &= [(\boldsymbol{\alpha} \cdot \mathbf{p}) \mathbf{R} - (\boldsymbol{\sigma} \cdot \mathbf{p})(\boldsymbol{\sigma} \cdot \mathbf{R}) \boldsymbol{\alpha}] \\ &\quad + [\mathbf{R}(\boldsymbol{\alpha} \cdot \mathbf{p}) - \boldsymbol{\alpha}(\boldsymbol{\sigma} \cdot \mathbf{R})(\boldsymbol{\sigma} \cdot \mathbf{p})] \end{aligned} \quad (\text{B6})$$

$$+ i \{ \boldsymbol{\sigma} \cdot (\mathbf{p} \times \mathbf{R}) \boldsymbol{\alpha} + \boldsymbol{\alpha} [\boldsymbol{\sigma} \cdot (\mathbf{R} \times \mathbf{p})] \} \quad (\text{B7})$$

$$\begin{aligned} &= (\boldsymbol{\alpha} \cdot \mathbf{p}) [\mathbf{R} - (\boldsymbol{\sigma} \cdot \mathbf{R}) \boldsymbol{\sigma}] + [\mathbf{R} - \boldsymbol{\sigma}(\boldsymbol{\sigma} \cdot \mathbf{R})] (\boldsymbol{\alpha} \cdot \mathbf{p}) \\ &\quad + \frac{i}{r^3} [\boldsymbol{\alpha}(\boldsymbol{\sigma} \cdot \mathbf{l}) - (\boldsymbol{\sigma} \cdot \mathbf{l}) \boldsymbol{\alpha}]. \end{aligned} \quad (\text{B8})$$

A factor of γ_5 has been moved through the brackets so that the first two operators are proportional to $(\boldsymbol{\alpha} \cdot \mathbf{p})$, rather than to mixtures involving $(\boldsymbol{\sigma} \cdot \mathbf{p})$. The effect of this is to change the free factors of $\boldsymbol{\alpha}$ to free factors of $\boldsymbol{\sigma}$ in the first two brackets.

We now assume that we require only the expectation value of this operator in an eigenfunction of the Dirac Hamiltonian of the form

$$[c(\boldsymbol{\alpha} \cdot \mathbf{p}) + \beta m c^2 + V(\mathbf{r})] |\psi\rangle = E |\psi\rangle, \quad (\text{B9})$$

so that, for eigenfunctions of this operator equation, we can write

$$(\boldsymbol{\alpha} \cdot \mathbf{p}) |\psi\rangle = \frac{1}{c} [E - \beta m c^2 - V(\mathbf{r})] |\psi\rangle. \quad (\text{B10})$$

The operator $\mathcal{E} = (E - \beta m c^2 - V)$ commutes with both $\boldsymbol{\sigma}$ and \mathbf{R} , and the expectation value of the first two terms in the operator may be written, by virtue of the commutation of the operators, as

$$\begin{aligned} \langle \mathcal{E} [2\mathbf{R} - (\boldsymbol{\sigma} \cdot \mathbf{R}) \boldsymbol{\sigma} - \boldsymbol{\sigma}(\boldsymbol{\sigma} \cdot \mathbf{R})] \rangle &= \langle \mathcal{E} [2\mathbf{R} - \mathbf{R} - i(\boldsymbol{\sigma} \times \mathbf{R}) - \mathbf{R} \\ &\quad + i(\boldsymbol{\sigma} \times \mathbf{R})] \rangle = 0. \end{aligned} \quad (\text{B11})$$

Only the third part of the complete operator has a nonzero expectation value, which may be written

$$- \frac{i \gamma_5}{r^3} \{ [l - i(\boldsymbol{\sigma} \times \mathbf{l})] - [l + i(\boldsymbol{\sigma} \times \mathbf{l})] \} = \frac{2}{r^3} (\boldsymbol{\alpha} \times \mathbf{l}), \quad (\text{B12})$$

in agreement with the result in Ref. [19].

The approximation arises because we assume that the eigenstates are simultaneous solutions of the Dirac equation for a local single-particle potential, $V(\mathbf{r})$. In fact, we could have terms involving pairs of electrons and mixed electron coordinates $\{i, j\}$. Mårtensson-Pendrill discusses this in her review article [55], and notes that such effects are generally small in the related hyperfine interaction problem, and can be neglected.

-
- [1] P. A. M. Dirac, *Rev. Mod. Phys.* **21**, 392 (1949).
 [2] E. M. Purcell and N. F. Ramsey, *Phys. Rev.* **78**, 807 (1950).
 [3] T. D. Lee and C. N. Yang, *Phys. Rev.* **105**, 1671 (1957).
 [4] C. S. Wu, E. Ambler, R. W. Hayward, D. D. Hoppes, and R. P. Hudson, *Phys. Rev.* **105**, 1413 (1957).
 [5] R. P. Feynman and M. Gell-Mann, *Phys. Rev.* **109**, 193 (1958).
 [6] S. L. Glashow, *Nucl. Phys.* **22**, 579 (1961).
 [7] S. Weinberg, *Phys. Rev. Lett.* **19**, 1264 (1967).

- [8] A. Salam, in *Nobel Symposium*, edited by N. Svartholm (Almqvist and Wiksell, Stockholm, 1968), Vol. 8.
 [9] P. G. H. Sandars, *Phys. Scr.* **36**, 904 (1987).
 [10] P. G. H. Sandars, *Phys. Scr.* **T46**, 16 (1993).
 [11] W. R. Johnson, J. Sapirstein, and S. A. Blundell, *Phys. Scr.* **T46**, 184 (1993).
 [12] C. S. Wood, S. C. Bennett, D. Cho, B. P. Masterson, J. L. Roberts, C. E. Tanner, and C. E. Wieman, *Science* **275**, 1759 (1997).

- [13] J. H. Christenson, J. W. Cronin, V. L. Fitch, and R. Turlay, *Phys. Rev. Lett.* **13**, 138 (1964).
- [14] E. D. Commins and P. H. Bucksbaum, *Weak Interactions of Leptons and Quarks* (Cambridge University Press, Cambridge, 1983).
- [15] L. I. Schiff, *Phys. Rev.* **132**, 2194 (1963).
- [16] P. G. H. Sandars, *Phys. Rev. Lett.* **19**, 1396 (1967).
- [17] G. E. Harrison, P. G. H. Sandars, and S. J. Wright, *Phys. Rev. Lett.* **22**, 1263 (1969).
- [18] E. A. Hinds, C. E. Loving, and P. G. H. Sandars, *Phys. Lett. B* **62**, 97 (1976).
- [19] E. A. Hinds and P. G. H. Sandars, *Phys. Rev. A* **21**, 471 (1980).
- [20] E. A. Hinds and P. G. H. Sandars, *Phys. Rev. A* **21**, 480 (1980).
- [21] P. V. Coveney and P. G. H. Sandars, *J. Phys. B* **16**, 3727 (1983).
- [22] D. A. Wilkening, N. F. Ramsey, and D. J. Larson, *Phys. Rev. A* **29**, 425 (1984).
- [23] D. Cho, K. Sangster, and E. A. Hinds, *Phys. Rev. Lett.* **63**, 2559 (1989).
- [24] D. Cho, K. Sangster, and E. A. Hinds, *Phys. Rev. A* **44**, 2783 (1991).
- [25] V. V. Flambaum, I. B. Khriplovich, and O. P. Sushkov, *Nucl. Phys. A* **449**, 750 (1986).
- [26] F. A. Parpia, *J. Phys. B* **30**, 3983 (1997).
- [27] J. K. Laerdahl, T. Saue, K. Fægri, Jr., and H. M. Quiney, *Phys. Rev. Lett.* **79**, 1642 (1997).
- [28] E. E. Salpeter, *Phys. Rev.* **112**, 1642 (1958).
- [29] E. Lindroth, B. W. Lynn, and P. G. H. Sandars, *J. Phys. B* **22**, 559 (1989).
- [30] J. D. Bjorken and S. D. Drell, *Relativistic Quantum Mechanics* (McGraw-Hill, New York, 1964).
- [31] O. P. Sushkov, V. V. Flambaum, and I. B. Khriplovich, *Zh. Éksp. Teor. Fiz.* **87**, 1521 (1984) [*Sov. Phys. JETP* **60**, 873 (1984)].
- [32] I. P. Grant and H. M. Quiney, *Adv. At. Mol. Phys.* **23**, 37 (1988).
- [33] K. G. Dyall, K. Fægri, Jr., and P. R. Taylor, in *The Effects of Relativity in Atoms, Molecules and the Solid State*, edited by S. Wilson, I. P. Grant, and B. L. Gyorffy (Plenum, New York, 1991).
- [34] M. Synek, *Phys. Rev.* **136**, 1552 (1964).
- [35] Y.-K. Kim, *Phys. Rev.* **154**, 17 (1967).
- [36] H. M. Quiney, I. P. Grant, and S. Wilson, *J. Phys. B* **20**, 1413 (1987).
- [37] H. M. Quiney, H. Skaane, and I. P. Grant, *J. Phys. B* (to be published).
- [38] T. Saue, K. Fægri, Jr., T. Helgaker, and O. Gropen, *Mol. Phys.* **91**, 937 (1997).
- [39] H. M. Quiney, H. Skaane, and I. P. Grant, *Adv. Quantum Chem.* (to be published).
- [40] K. G. Dyall and K. Fægri, Jr., *Chem. Phys. Lett.* **174**, 25 (1990).
- [41] R. Stanton and S. Havriliak, *J. Chem. Phys.* **81**, 1910 (1984).
- [42] E. U. Condon and G. H. Shortley, *The Theory of Atomic Spectra* (Cambridge University Press, Cambridge, 1935).
- [43] DALTON, an electronic structure program, Release 1.0 (1997), written by T. Helgaker, H. J. Aa. Jensen, P. Jørgensen, J. Olsen, K. Ruud, H. Ågren, T. Andersen, K. L. Bak, V. Bakken, O. Christiansen, P. Dahle, E. K. Dalskov, T. Enevoldsen, B. Fernandez, H. Heiberg, H. Hettema, D. Jonsson, S. Kirpekar, R. Kobayashi, H. Koch, K. V. Mikkelsen, P. Norman, M. J. Packer, T. Saue, P. R. Taylor, and O. Vahtras.
- [44] V. R. Saunders, in *Methods of Computational Molecular Physics*, edited by G. H. F. Diercksen and S. Wilson (Reidel, Dordrecht, 1983).
- [45] T. U. Helgaker and P. R. Taylor, in *Modern Electronic Structure Theory*, edited by D. R. Yarkony (World Scientific, Singapore, 1995), Pt. II.
- [46] R. McWeeny, *Methods of Molecular Quantum Mechanics*, 2nd ed. (Academic, London, 1992), p. 38.
- [47] K. G. Dyall, I. P. Grant, C. T. Johnson, F. A. Parpia, and E. P. Plummer, *Comput. Phys. Commun.* **55**, 425 (1989).
- [48] K. G. Dyall and K. Fægri, Jr., *Theor. Chim. Acta* **94**, 39 (1996).
- [49] J. K. Laerdahl, T. Saue, and K. Fægri, Jr., *Theor. Chem. Acc.* **97**, 177 (1997).
- [50] P. Pulay, in *Modern Theoretical Chemistry*, edited by H. F. Schaefer III (Plenum, New York, 1977), Vol. 4.
- [51] J. Almlöf and T. Helgaker, *Chem. Phys. Lett.* **83**, 125 (1981).
- [52] I. B. Khriplovich, *Parity Nonconservation in Atomic Phenomena* (Gordon and Breach, Philadelphia, 1991).
- [53] H. M. Quiney, H. Skaane, and I. P. Grant, *J. Phys. B* (to be published).
- [54] V. V. Flambaum and I. B. Khriplovich, *Zh. Éksp. Teor. Fiz.* **89**, 1505 (1985) [*Sov. Phys. JETP* **62**, 872 (1985)].
- [55] A. M. Mårtensson-Pendrill, in *Methods in Computational Chemistry V: Atomic and Molecular Properties*, edited by S. Wilson (Plenum, New York, 1992).
- [56] B. E. Sauer, J. Wang, and E. A. Hinds, *Phys. Rev. Lett.* **74**, 1554 (1995).
- [57] J. Almlöf, K. Fægri, Jr., and K. Korsell, *J. Comput. Chem.* **3**, 385 (1982).
- [58] L. Visscher, T. J. Lee, and K. G. Dyall, *J. Chem. Phys.* **105**, 8769 (1996).
- [59] H. M. Quiney, H. Skaane, and I. P. Grant, *Chem. Phys. Lett.* (to be published).
- [60] M. G. Kozlov and L. N. Labzowsky, *J. Phys. B* **28**, 1933 (1995).
- [61] E. A. Hinds, Ph.D. thesis, University of Oxford, 1982 (unpublished).
- [62] K. P. Huber and G. Herzberg, *Molecular Spectra and Molecular Structure IV. Constants of Diatomic Molecules* (Litton, New York, 1979).